Unveiling distinguishable non-Gaussian quantum states

Andrea Giani [1], Moe Z. Win [2,*], Peter L. Falb [2], and Andrea Conti [1,†]
[1] *Department of Engineering and CNIT, University of Ferrara, 44122 Ferrara, Italy*
[2] *Laboratory for Information and Decision Systems, Massachusetts Institute of Technology, Cambridge, Massachusetts 02139, USA*

(Received 16 April 2025; accepted 9 January 2026; published 15 June 2026)

Quantum systems promise unprecedented performance with respect to classical counterparts for various applications involving sensing, communications, control, and computing. Bringing this promise to reality hinges upon the distinguishability between quantum states. This paper explores the distinguishability of a broad class of non-Gaussian states, namely the photon-varied Gaussian states (PVGSs), which can be generated with current technologies from Gaussian states of the electromagnetic field. First, we show that the problem of designing orthogonal PVGSs is tantamount to determining the algebraic varieties of generalized Hermite polynomials, thus bridging the fields of quantum mechanics and algebraic geometry. Then, we prove the existence of orthogonal PVGSs by showing that proper choices of the states' parameters lead to nonempty algebraic varieties. By exploiting the geometrical properties of such algebraic varieties, we also establish methodologies for designing pairs of orthogonal PVGSs. Finally, we explore the distinguishability of PVGSs undergoing noisy time evolution in the presence of decoherence and show that, in such conditions, the developed methodologies still allow for achieving the highest distinguishability. By bridging quantum mechanics and algebraic geometry, the findings of this paper provide insights into designing a new class of quantum states that are distinguishable.

DOI: 10.1103/ffbg-4897

I. INTRODUCTION

The quantum-mechanical description of the electromagnetic field and its tight interplay with information theory enable the design of quantum systems that involve sensing, communications, control, and computing. Such systems exploit quantum states to accomplish their tasks. Therefore, the systems' performance depends on the properties of the employed quantum states, including their distinguishability. Such distinguishability, the degree with which the states can be discriminated, is quantified by their inner product. Gaussian states have been extensively employed in quantum systems owing to the possibility of manipulating them with current optical setups and to their well-established theoretical foundations [1–3]. However, Gaussian states exhibit two major drawbacks that affect quantum systems' performance: they possess limited nonclassical properties and they are nonorthogonal, causing an unavoidable error when attempting to distinguish them. Mitigating such limitations motivates the investigation of non-Gaussian states [4].

State of the art. Non-Gaussian states are considered suitable candidates for overcoming the limitations of Gaussian states. Their name is attributed to the fact that, unlike Gaussian states, their Wigner function is not Gaussian [4]. Since the class of non-Gaussian states is vast, establishing a well-defined structure is arduous. The main criteria used to accomplish this task are based on the stellar characterization [5,6] and on signatures of nonclassicality, e.g., Wigner function negativity [7]. Considerable research efforts have been devoted to studying different classes of non-Gaussian states, including Gottesman-Kitaev-Preskill (GKP) states, Schrödinger cat states, and photon-varied Gaussian states (PVGSs). While GKP states [8], initially conceived to encode a qubit in a harmonic oscillator, cannot be physically realized, an approximation of them can be implemented via nonorthogonal Gaussian-enveloped squeezed displaced states [9]. Likewise, both Schrödinger cat states and PVGSs can be generated using current technologies. Specifically, Schrödinger cats are obtained as a superposition of opposite-phase quantum coherent states [10–12], whereas PVGSs are generated by annihilating or exciting photons from initial Gaussian states of the electromagnetic field [13–15]. Interestingly, optical implementations of Schrödinger cats can be accomplished via annihilation of photons from squeezed vacuum states [12,16]. To this extent, Schrödinger cats can be regarded as a subclass of PVGSs. Therefore, PVGSs form a rich class of non-Gaussian states. In the literature, PVGSs have been characterized based on their quantum characteristic functions [15,17,18], their non-Gaussian behavior [17–20], and their Fock representation and orthogonality [13]. The high interest in PVGSs is mainly attributed to two aspects. First, they can be generated from Gaussian states with current technologies [21–26]; thus they are easier to prepare than other non-Gaussian states. Second, they can outperform the Gaussian states in a variety of applications [13,14,27–35]. Although PVGSs can alleviate

*Also at Quantum neXus Laboratory; Institute for Data, Systems, and Society; Department of Aeronautics and Astronautics; Schwarzman College of Computing; and Institute for Soldier Nanotechnologies.
†Contact author: andrea.conti@unife.it

the limited nonclassicality of Gaussian states, it is still unclear to what extent their quantum nature affects their distinguishability.

Contributions of the paper. The inner product between PVGSs can be derived in closed forms involving generalized Hermite–Kampé de Fériet (HKdF) polynomials. Consequently, two central questions arise: (i) can the properties of such polynomials be leveraged to gain insights into the distinguishability of PVGSs; and (ii) can these insights lead to design methodologies that make such states distinguishable, even in the presence of noise? The answers to these questions will lead to a new class of quantum states of the electromagnetic field that are distinguishable.

This paper explores the quantum distinguishability of a broad class of non-Gaussian states, namely, the PVGSs. The key idea of this paper is as follows. We show that the inner product between PVGSs is proportional to generalized HKdF polynomials. The roots of such polynomials form algebraic varieties and are of crucial importance as they annihilate the inner product between PVGSs. Hence, the problem of designing orthogonal PVGSs can be translated to that of determining algebraic varieties of generalized HKdF polynomials, thus bridging quantum mechanics and algebraic geometry. By exploring this connection, we establish methodologies for designing pairs of orthogonal PVGSs. The main contributions of this paper are as follows.

(i) We translate the problem of designing orthogonal PVGSs to that of determining algebraic varieties of generalized HKdF polynomials.

(ii) We prove the existence of orthogonal PVGSs by showing that proper choices of their parameters lead to nonempty algebraic varieties.

(iii) We exploit the geometrical properties of such algebraic varieties to establish methodologies for designing orthogonal PVGSs.

(iv) We explore the distinguishability of PVGSs undergoing noisy time evolution in the presence of quantum decoherence.

The remaining sections are organized as follows. Section II provides useful preliminaries on generalized classes of Hermite polynomials and on both Gaussian states and PVGSs. Section III presents simple orthogonalization problems involving a PVGS and proves the existence of orthogonal PVGSs. Section IV studies the geometrical properties of algebraic varieties associated with the inner product between PVGSs and establishes methodologies to design orthogonal PVGSs. Section V determines how noisy time evolution affects the distinguishability of PVGSs in the presence of dephasing. Section VI provides a summary and discusses our conclusions.

Notation. Vectors are denoted by bold lowercase letters. Matrices and operators are denoted by bold uppercase letters. The sets of natural numbers, integer numbers, real numbers, strictly negative real numbers, complex numbers, and nonzero complex numbers are denoted by $\mathbb{N}$, $\mathbb{Z}$, $\mathbb{R}$, $\mathbb{R}_-$, $\mathbb{C}$, and $\mathbb{C}_*$, respectively. All other sets are denoted by upright sans serif font. For $n \in \mathbb{Z}$, $\overline{n}| = -$ for $n < 0$ and $\overline{n}| = +$ for $n \geqslant 0$. For $x \in \mathbb{R}$, $\lfloor x \rfloor$ denotes the greatest integer less than or equal to x. For $z \in \mathbb{C}$, $|z|$ denotes its absolute value, $\angle z \in (-\pi, \pi]$ denotes its angle, z^* denotes its complex conjugate, and $\imath = \sqrt{-1}$. For $z \in \mathbb{C}$, the principal branch of the complex square root is chosen such that $\sqrt{z} = |z|^{1/2} \exp\{\imath(\angle z)/2\}$. For a function f, $\mathrm{Dom}(f)$ denotes its domain, $\mathrm{Ran}(f)$ denotes its range, and $f|_\Omega$ denotes the restriction of f to $\Omega \subseteq \mathrm{Dom}(f)$. For a matrix $\boldsymbol{M}$, $[\boldsymbol{M}]_{ij}$ denotes the element in the ith row and jth column. The adjoint of an operator is denoted by $(\cdot)^\dagger$. The annihilation and the creation operators are denoted by $\boldsymbol{A}$ and $\boldsymbol{A}^\dagger$, respectively. The identity operator defined on a Hilbert space $\mathcal{H}$ is denoted by $\boldsymbol{I}_\mathcal{H}$. For two operators $\boldsymbol{X}$ and $\boldsymbol{Y}$, the anticommutator and commutator of $\boldsymbol{X}$ and $\boldsymbol{Y}$ are denoted by $[\![\boldsymbol{X}, \boldsymbol{Y}]\!]_\pm = \boldsymbol{XY} \pm \boldsymbol{YX}$ with $+$ or $-$, respectively. The displacement operator with parameter $\mu \in \mathbb{C}$ is denoted by $\boldsymbol{D}_\mu \triangleq \exp\{\mu\boldsymbol{A}^\dagger - \mu^*\boldsymbol{A}\}$. The squeezing operator with parameter $\zeta \in \mathbb{C}$ is denoted by $\boldsymbol{S}_\zeta \triangleq \exp\{\frac{1}{2}\zeta(\boldsymbol{A}^\dagger)^2 - \frac{1}{2}\zeta^*\boldsymbol{A}^2\}$.

II. PRELIMINARIES

This section provides preliminaries on Hermite polynomials and their generalizations, as well as on single-mode Gaussian states and single-mode PVGSs.

A. Hermite polynomials and their generalizations

Hermite polynomials and their generalizations will play a fundamental role in the following. We now recall single-variable and two-variable Hermite polynomials and discuss two useful generalizations, namely, bivariate hypergeometric Hermite polynomials and HKdF polynomials.

Letting $x, y \in \mathbb{C}$ and $n \in \mathbb{N}$, the single-variable and two-variable Hermite polynomials are defined as

$$H_n(x) \triangleq n! \sum_{k=0}^{\lfloor n/2 \rfloor} \frac{(-1)^k}{k!(n-2k)!}(2x)^{n-2k}, \tag{1}$$

$$H_n(x, y) \triangleq n! \sum_{k=0}^{\lfloor n/2 \rfloor} \frac{1}{k!(n-2k)!} x^{n-2k} y^k, \tag{2}$$

respectively. Note that (1) and (2) are related to each other by $H_n(x) = H_n(2x, -1)$.

Hypergeometric bivariate Hermite polynomials form a class of generalized polynomials defined as [36]

$$\mathscr{H}_{m,n}(x, y|\boldsymbol{\Theta}) \triangleq \sum_{k=0}^{\min\{m,n\}} (-[\boldsymbol{\Theta}]_{12})^k k! \binom{m}{k}\binom{n}{k} \left(\frac{[\boldsymbol{\Theta}]_{11}}{2}\right)^{(m-k)/2} \left(\frac{[\boldsymbol{\Theta}]_{22}}{2}\right)^{(n-k)/2} H_{m-k}\left(\frac{[\boldsymbol{\Theta}]_{11}x + [\boldsymbol{\Theta}]_{12}y}{\sqrt{2[\boldsymbol{\Theta}]_{11}}}\right)$$
$$\times H_{n-k}\left(\frac{[\boldsymbol{\Theta}]_{12}x + [\boldsymbol{\Theta}]_{22}y}{\sqrt{2[\boldsymbol{\Theta}]_{22}}}\right), \tag{3}$$

where $x, y \in \mathbb{C}$, $m, n \in \mathbb{N}$, and $\boldsymbol{\Theta} \in \mathbb{C}_*^{2\times 2}$ is a nonsingular matrix shaping the expansion of $\mathscr{H}_{m,n}(x, y|\boldsymbol{\Theta})$. Using $\boldsymbol{\Theta}$ to define the affine transformation

$$\breve{x} \triangleq \frac{[\boldsymbol{\Theta}]_{11}x + [\boldsymbol{\Theta}]_{12}y}{\sqrt{[\boldsymbol{\Theta}]_{11}}}, \quad \breve{y} \triangleq \frac{[\boldsymbol{\Theta}]_{12}x + [\boldsymbol{\Theta}]_{22}y}{\sqrt{[\boldsymbol{\Theta}]_{22}}}$$

allows one to define the affine hypergeometric bivariate Hermite polynomials as

$$\breve{\mathscr{H}}_{m,n}(\breve{x}, \breve{y}|\boldsymbol{\Theta}) \triangleq \sum_{k=0}^{\min\{m,n\}} (-[\boldsymbol{\Theta}]_{12})^k k! \binom{m}{k}\binom{n}{k}\left(\frac{[\boldsymbol{\Theta}]_{11}}{2}\right)^{(m-k)/2}\left(\frac{[\boldsymbol{\Theta}]_{22}}{2}\right)^{(n-k)/2} H_{m-k}\left(\frac{\breve{x}}{\sqrt{2}}\right)H_{n-k}\left(\frac{\breve{y}}{\sqrt{2}}\right). \tag{4}$$

Generalized HKdF polynomials are another class of generalized polynomials defined as [37,38]

$$H_{m,n}(x, y; z, u\,|t) \triangleq \sum_{k=0}^{\min\{m,n\}} t^k k! \binom{m}{k}\binom{n}{k} \times H_{m-k}(x, y)H_{n-k}(z, u), \tag{5}$$

where $x, y, z, u, t \in \mathbb{C}$ and $m, n \in \mathbb{N}$. To facilitate the derivation and manipulation of analytical expressions for the PVGSs, it is useful to define the function

$$G_{m,n}(x, y|\alpha, \beta) \triangleq \frac{1}{(1-\alpha^2)^{(m+n)/2}} M(x, y|\alpha) \times H_{m,n}\left(\frac{2(x-y\alpha)}{\sqrt{1-\alpha^2}}, -1; \frac{2(y-x\alpha)}{\sqrt{1-\alpha^2}}, -1\middle|2\beta\right), \tag{6}$$

where $x, y, \alpha, \beta \in \mathbb{C}$, $\alpha \neq 1$, $m, n \in \mathbb{N}$, and $M(x, y|\alpha)$ is the Mehler formula [39]

$$M(x, y|\alpha) \triangleq \sum_{k=0}^{\infty} \frac{\alpha^k}{2^k k!} H_k(x)H_k(y) \tag{7a}$$

$$= \frac{1}{\sqrt{1-\alpha^2}} \exp\left(\frac{2xy\alpha - (x^2+y^2)\alpha^2}{1-\alpha^2}\right). \tag{7b}$$

B. Single-mode bosonic quantum field

Characterizing the distinguishability between quantum states requires considering the quantum-mechanical description of the electromagnetic field. Such a description originates from the second quantization [40], which typically considers an initial classical transversal field (governed by Maxwell's equations and Coulomb's gauge) localized in a cubical region and obeying periodic boundary conditions. Plane-wave modal decomposition, i.e., three-dimensional spatial Fourier expansion, reveals that the electromagnetic field is an infinite discrete superposition of monochromatic radiations, referred to as modes, each one identified by a pair $(\boldsymbol{k}, \boldsymbol{e}_{\boldsymbol{k},\lambda})$, where $\boldsymbol{k}$ and $\boldsymbol{e}_{\boldsymbol{k},\lambda}$ are the wave and polarization vector, respectively, with $\lambda = 0, 1$. The harmonic behavior of each mode leads the field to be considered as an ensemble of independent harmonic oscillators. Therefore, the electromagnetic field is quantized by conversion of each harmonic oscillator to its quantum-mechanical counterpart.[1] The quantization procedure consists of defining, for each harmonic oscillator, a pair of operators $\boldsymbol{A}_{\boldsymbol{k},\lambda}$ and $\boldsymbol{A}_{\boldsymbol{k},\lambda}^\dagger$ referred to as bosonic annihilation and creation operators, respectively, which satisfy the commutation relations $[\![\boldsymbol{A}_{\boldsymbol{k},\lambda}, \boldsymbol{A}_{\boldsymbol{k}',\lambda'}]\!]_- = 0$ and $[\![\boldsymbol{A}_{\boldsymbol{k},\lambda}, \boldsymbol{A}_{\boldsymbol{k}',\lambda'}^\dagger]\!]_- = \delta_{\boldsymbol{k},\boldsymbol{k}'}\delta_{\lambda,\lambda'}\boldsymbol{I}_{\mathcal{H}}$, with $\mathcal{H}$ denoting the Hilbert space of the quantized field. When only one mode is excited, the field is referred to as single-mode bosonic quantum field and its states are called single-mode quantum states. In the following, we will focus on a single-mode bosonic field with arbitrary $(\boldsymbol{k}, \boldsymbol{e}_{\boldsymbol{k},\lambda})$ and, for notational simplicity, the dependence on $(\boldsymbol{k}, \boldsymbol{e}_{\boldsymbol{k},\lambda})$ will be dropped so that the associated operators $\boldsymbol{A}_{\boldsymbol{k},\lambda}$ and $\boldsymbol{A}_{\boldsymbol{k},\lambda}^\dagger$ will be simply denoted by $\boldsymbol{A}$ and $\boldsymbol{A}^\dagger$. The quadrature operators of the single-mode quantum field are defined as $\boldsymbol{Q} \triangleq (\boldsymbol{A} + \boldsymbol{A}^\dagger)/\sqrt{2}$ and $\boldsymbol{P} \triangleq \imath(\boldsymbol{A}^\dagger - \boldsymbol{A})/\sqrt{2}$ so that they satisfy the commutation relation $[\![\boldsymbol{Q}, \boldsymbol{P}]\!]_- = \imath\boldsymbol{I}_{\mathcal{H}}$. Unlike $\boldsymbol{A}$ and $\boldsymbol{A}^\dagger$, the operator $\boldsymbol{A}^\dagger\boldsymbol{A}$ is self-adjoint and its eigenvalues and eigenvectors are related by

$$\boldsymbol{A}^\dagger\boldsymbol{A}|n\rangle = n|n\rangle,$$

where $|n\rangle$, for $n \geqslant 0$, is the Fock state with exactly n photons. When $n = 0$, no photons are excited and the Fock state $|0\rangle$, referred to as the vacuum state, possesses the lowest possible energy level. Fock states form a complete and countable orthonormal basis for $\mathcal{H}$, meaning that any quantum state can be expanded with respect to such a basis. The Hilbert space $\mathcal{H}$ associated with the single-mode bosonic quantum field is equipped with an inner product structure described by the mapping

$$\langle\cdot,\cdot\rangle : \mathcal{H} \times \mathcal{H} \to \mathbb{C},$$
$$(|\phi\rangle, |\psi\rangle) \mapsto \langle|\phi\rangle, |\psi\rangle\rangle,$$

which, according to Dirac's formalism, can be written as $\langle|\phi\rangle, |\psi\rangle\rangle = \langle\psi|\phi\rangle$.[2] Thus, for each state (ket) $|\psi\rangle$, there exists a unique corresponding linear functional (bra) $\langle\psi| \in \mathcal{H}^*$, where $\mathcal{H}^*$ is the dual space of $\mathcal{H}$, whose application to a quantum state $|\phi\rangle$ defines $\langle\psi|\phi\rangle$. The correspondence between each state and its linear functional is independent of any choice of basis and from Riesz's representation theorem $\mathcal{H}$ and $\mathcal{H}^*$ are canonically isomorphic. The inner product is fundamental to defining the concept of distinguishability between quantum states.

[1] The quantization in free space is obtained by letting the size of the cubical region approach infinity. In such a case, the plane-wave modal decomposition leads to an integral representation of the field as modes are no longer discretized.

[2] Note that $\langle\cdot,\cdot\rangle$ ($\langle\cdot|\cdot\rangle$) is linear (antilinear) in the first component and antilinear (linear) in the second component.

Definition 1 (quantum distinguishability in $\mathcal{H}$). Two quantum states $|\psi\rangle, |\phi\rangle \in \mathcal{H}$ are distinguishable if $\langle\psi|\phi\rangle = 0$. Consequently, nonorthogonal quantum states are not distinguishable. □

C. Gaussian states

Single-mode Gaussian states are a class of quantum states that exhibit a Gaussian Wigner function. These states are widely employed in many quantum systems owing to consolidated theoretical foundations and adequate maturity of current technologies. Consider a Gaussian state defined as $|\mu,\zeta\rangle \triangleq \boldsymbol{D}_\mu \boldsymbol{S}_\zeta |0\rangle \in \mathcal{H}$.[3] Its expansion with respect to the Fock basis is given by [13]

$$|\mu,\zeta\rangle = \Lambda(\mu,\zeta)\sum_{n=0}^{\infty}\frac{1}{\sqrt{n!}}\left(-\frac{\tanh(|\zeta|)e^{\iota\angle\zeta}}{2}\right)^{n/2} \times H_n(\eta(\mu,\zeta))|n\rangle, \tag{8}$$

where

$$\Lambda(\mu,\zeta) \triangleq \sqrt{\operatorname{sech}(|\zeta|)} \times \exp\left\{-\frac{1}{2}(|\mu|^2 - (\mu^*)^2\tanh(|\zeta|)e^{\iota\angle\zeta})\right\}, \tag{9}$$

$$\eta(\mu,\zeta) \triangleq \frac{\mu - \mu^*\tanh(|\zeta|)e^{\iota\angle\zeta}}{\sqrt{-2\tanh(|\zeta|)e^{\iota\angle\zeta}}}. \tag{10}$$

Given two Gaussian states $|\xi,\omega\rangle, |\mu,\zeta\rangle \in \mathcal{H}$, their inner product can be determined by using their Fock representation (8) and the Mehler formula (7) as

$$\langle\omega,\xi|\mu,\zeta\rangle = \Lambda(\xi,\omega)^*\Lambda(\mu,\zeta)\,M(\eta(\xi,\omega)^*,\eta(\mu,\zeta)|\rho(\omega,\zeta)),$$

where

$$\rho(\omega,\zeta) \triangleq \left(\sqrt{-\tanh(|\omega|)e^{\iota\angle\omega}}\right)^*\sqrt{-\tanh(|\zeta|)e^{\iota\angle\zeta}}. \tag{11}$$

Note that since (7) and (9) do not vanish at any point, $\langle\omega,\xi|\mu,\zeta\rangle$ is always nonzero, thus showing that Gaussian states are always nonorthogonal. Consequently, quantum systems relying on distinguishing Gaussian states are affected by an unavoidable error.

[3] In some papers, Gaussian states are also defined by swapping the squeezing and displacement operators. Such a definition is obtained from ours by applying a Bogoliubov-Valatin transformation to μ and ζ. Furthermore, note that Gaussian states are closed under rotational transformations and any rotation parameter can be taken into account by redefining μ and ζ.

D. Photon-varied Gaussian states

PVGSs are non-Gaussian states obtained by either annihilating (photon-subtracted Gaussian states (PSGSs)) or exciting (photon-added Gaussian states (PAGSs)) photons from initial Gaussian states of the quantized electromagnetic field. Photon-subtraction and photon-addition operations are unified by the photon-variation operator defined as

$$\boldsymbol{V}_{\bar{t}|} \triangleq \begin{cases} \boldsymbol{A} & \text{for} \quad t=-1 \text{ (photon subtraction)} \\ \boldsymbol{A}^\dagger & \text{for} \quad t=+1 \text{ (photon addition)}, \end{cases} \tag{12}$$

where $t \in \{-1,+1\}$ is the parameter that specifies the type of photon-variation operation to perform. Given a Gaussian state $|\mu,\zeta\rangle \in \mathcal{H}$, the corresponding PVGS is defined as

$$|\psi_{\bar{t}|}^{(k)}(\mu,\zeta)\rangle \triangleq \frac{1}{N_{\bar{t}|}^{(k)}}\boldsymbol{V}_{\bar{t}|}^{k}|\mu,\zeta\rangle \in \mathcal{H}, \tag{13}$$

where k is the number of photon-variation operations and $N_{\bar{t}|}^{(k)}$ denotes the associated normalization constant ensuring $|\psi_{\bar{t}|}^{(k)}(\mu,\zeta)\rangle$ has unit norm, required because $\boldsymbol{V}_{\bar{t}|}$ is a nonunitary operator. Therefore, the PVGS $|\psi_{\bar{t}|}^{(k)}(\mu,\zeta)\rangle$ has four parameters, namely t, k, μ, and ζ (see Fig. 1).

The expansion of $|\psi_{\bar{t}|}^{(k)}(\mu,\zeta)\rangle$ with respect to the Fock basis is given by [13]

$$|\psi_{\bar{t}|}^{(k)}(\mu,\zeta)\rangle = \frac{\Lambda(\mu,\zeta)}{N_{\bar{t}|}^{(k)}}\sum_{n=0}^{\infty}\sqrt{\frac{(n+k)!}{n!\left(n-k\frac{t-1}{2}\right)!}} \times\left(-\frac{\tanh(|\zeta|)e^{\iota\angle\zeta}}{2}\right)^{(1/2)[n-k(t-1)/2]} \times H_{n-k(t-1)/2}(\eta(\mu,\zeta))|n+k\frac{t+1}{2}\rangle. \tag{14}$$

Note that when $k=0$, i.e., no photon-variation operations are performed, the initial Gaussian state is kept untouched and (14) reduces to (8). Given two PVGSs $|\psi_{\bar{s}|}^{(h)}(\xi,\omega)\rangle, |\psi_{\bar{t}|}^{(k)}(\mu,\zeta)\rangle \in \mathcal{H}$, with $h \leqslant k$, their inner product $\langle\psi_{\bar{s}|}^{(h)}(\xi,\omega)|\psi_{\bar{t}|}^{(k)}(\mu,\zeta)\rangle$ is given by the closed-form expressions [13]

$$\langle\psi_{+}^{(h)}(\xi,\omega)|\psi_{+}^{(k)}(\mu,\zeta)\rangle = \frac{\Lambda(\xi,\omega)^*\Lambda(\mu,\zeta)}{N_{+}^{(h)}N_{+}^{(k)}}\left(\frac{\rho(\omega,\zeta)}{2}\right)^h\left[\left(-\frac{\tanh(|\omega|)e^{\iota\angle\omega}}{2}\right)^{(k-h)/2}\right]^* \times G_{k,h}(\eta(\xi,\omega)^*,\eta(\mu,\zeta)|\rho(\omega,\zeta),\rho(\omega,\zeta)^{-1}), \tag{15a}$$

$$\langle\psi_{+}^{(h)}(\xi,\omega)|\psi_{-}^{(k)}(\mu,\zeta)\rangle = \frac{\Lambda(\xi,\omega)^*\Lambda(\mu,\zeta)}{N_{+}^{(h)}N_{-}^{(k)}}\left(-\frac{\tanh(|\zeta|)\,e^{\iota\angle\zeta}}{2}\right)^{(h+k)/2} \times G_{0,h+k}(\eta(\xi,\omega)^*,\eta(\mu,\zeta)|\rho(\omega,\zeta),\rho(\omega,\zeta)), \tag{15b}$$

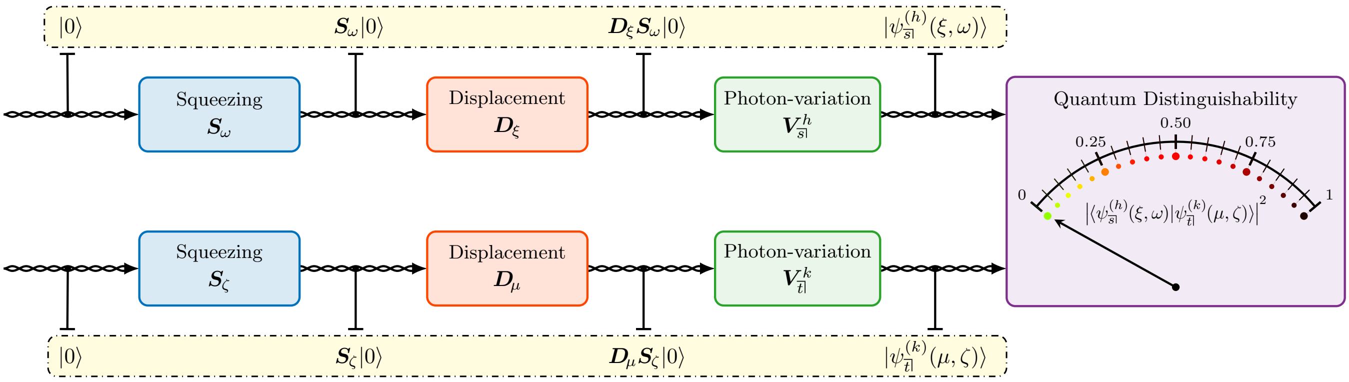

FIG. 1. Block diagram representing the sequence of operations to implement PVGSs and a measure of their quantum distinguishability obtained via inner product calculation. Such quantum distinguishability ranges from 0 (green circle) for orthogonal (distinguishable) PVGSs to 1 (black circle) for totally overlapping (indistinguishable) PVGSs.

$$\begin{aligned}\langle\psi_{-}^{(h)}(\xi,\omega)|\psi_{+}^{(k)}(\mu,\zeta)\rangle &= \frac{\Lambda(\xi,\omega)^*\Lambda(\mu,\zeta)}{N_{-}^{(h)}N_{+}^{(k)}}\left[\left(-\frac{\tanh(|\omega|)e^{\iota\angle\omega}}{2}\right)^{(h+k)/2}\right]^*\\ &\quad\times G_{h+k,0}(\eta(\xi,\omega)^*,\eta(\mu,\zeta)|\rho(\omega,\zeta),\rho(\omega,\zeta)), \end{aligned}\tag{15c}$$

$$\begin{aligned}\langle\psi_{-}^{(h)}(\xi,\omega)|\psi_{-}^{(k)}(\mu,\zeta)\rangle &= \frac{\Lambda(\xi,\omega)^*\Lambda(\mu,\zeta)}{N_{-}^{(h)}N_{-}^{(k)}}\left(\frac{\rho(\omega,\zeta)}{2}\right)^h\left(-\frac{\tanh(|\zeta|)e^{\iota\angle\zeta}}{2}\right)^{(k-h)/2}\\ &\quad\times G_{h,k}(\eta(\xi,\omega)^*,\eta(\mu,\zeta)|\rho(\omega,\zeta),\rho(\omega,\zeta))\end{aligned}\tag{15d}$$

for $(s,t)=(+1,+1)$, $(+1,-1)$, $(-1,+1)$, and $(-1,-1)$, respectively. Equations (15a)–(15d) show that, through (6), the inner product between two PVGSs depends on HKdF polynomials. Consequently, two central questions arise: (i) are there choices of PVGSs' parameters that annihilate such HKdF polynomials, thus making the states orthogonal; and (ii) if yes, how may such parameters be determined? The remainder of the paper studies the orthogonalization of PVGSs and answers such questions in order to obtain distinguishable non-Gaussian states.

III. ORTHOGONALIZATION OF PVGSS

A PVGS $|\psi_{\overline{t}|}^{(k)}(\mu,\zeta)\rangle\in\mathcal{H}$ can be regarded as the result of a mapping from the set of its parameters to the underlying Hilbert space of the associated single-mode bosonic quantum field, namely,

$$\begin{aligned}\Omega:\{-1,+1\}\times\mathbb{N}\times\mathbb{C}\times\mathbb{C}&\rightarrow\mathcal{H},\\ (t,k,\mu,\zeta)&\mapsto|\psi_{\overline{t}|}^{(k)}(\mu,\zeta)\rangle.\end{aligned}$$

Note that the inner product between two PVGSs $|\psi_{\overline{t}|}^{(k)}(\mu,\zeta)\rangle=\Omega(t,k,\mu,\zeta)$ and $|\psi_{\overline{s}|}^{(h)}(\xi,\omega)\rangle=\Omega(s,h,\xi,\omega)$ is

$$\begin{aligned}\langle|\psi_{\overline{t}|}^{(k)}(\mu,\zeta)\rangle,|\psi_{\overline{s}|}^{(h)}(\xi,\omega)\rangle\rangle&=\langle\Omega(t,k,\mu,\zeta),\Omega(s,h,\xi,\omega)\rangle\\ &=\langle\psi_{\overline{s}|}^{(h)}(\xi,\omega)|\psi_{\overline{t}|}^{(k)}(\mu,\zeta)\rangle.\end{aligned}$$

It follows that if there exist PVGSs' parameters annihilating (15a)–(15d) for $(s,t)=(+1,+1)$, $(+1,-1)$, $(-1,+1)$, and $(-1,-1)$, respectively, then they are the ones to use for the design of orthogonal PVGSs.

A. Simple orthogonalization problems

Before discussing the general orthogonalization problem for two PVGSs, we consider two simple problems.

(i) Orthogonalization of a PVGS and a Fock state. Consider a PVGS $|\psi_{\overline{t}|}^{(k)}(\mu,\zeta)\rangle\in\mathcal{H}$ and the Fock state with n photons $|n\rangle$. From (14) and the orthonormality of the Fock states, the orthogonalization condition $\langle n|\psi_{\overline{t}|}^{(k)}(\mu,\zeta)\rangle=0$ requires satisfying

$$H_{n+k}(\eta(\mu,\zeta))=0\quad\text{for } t=-1,\tag{16a}$$

$$H_{n-k}(\eta(\mu,\zeta))=0\quad\text{for } t=+1,\quad n>k,\tag{16b}$$

which occurs when the displacement μ and squeezing ζ parameters are chosen such that $\eta(\mu,\zeta)$ falls into a root of the corresponding single-variable Hermite polynomial. Note that when $t=+1$, the PAGS $|\psi_{+}^{(k)}(\mu,\zeta)\rangle$ is never orthogonal to the Fock state $|k\rangle$ as $\langle k|\psi_{+}^{(k)}(\mu,\zeta)\rangle\propto H_0(\eta(\mu,\zeta))=1$. In addition, $|\psi_{+}^{(k)}(\mu,\zeta)\rangle$ is orthogonal to the subspace $\text{span}(\{|n\rangle\}_{n<k})$ spanned by the Fock states with $n<k$ photons.

Remark 1. In various applications, e.g., quantum illumination, sub-Poissonian quantum imaging, and quantum communications, it is important to design a quantum light source that produces quantum states that are distinguishable from the vacuum state $|0\rangle$. From (16) with $n=0$, it follows that, unlike Gaussian states, the PVGSs can be designed to achieve orthogonality with respect to the vacuum state $|0\rangle$. While the orthogonality is automatically achieved by PAGSs, for PSGSs μ and ζ must be chosen such that $\eta(\mu,\zeta)$ falls into one of the k roots of the single-variable Hermite polynomial $H_k(x)$.[4] Notice that this requires $\zeta \neq 0$ as the photon subtraction does not alter coherent states, which are never orthogonal to $|0\rangle$. Indeed, for $\zeta = 0$, $|\psi_-^{(k)}(\mu, 0)\rangle = e^{\imath k \angle \mu}|\mu, 0\rangle$, thus leading to $\langle 0|\psi_-^{(k)}(\mu, 0)\rangle = e^{\imath k\angle\mu - |\mu|^2/2} \neq 0$ for all $\mu \in \mathbb{C}$. □

(ii) Orthogonalization of a single-PVGS and a Gaussian state. Consider a single-PVGS $|\psi_{\overline{t|}}^{(1)}(\mu,\zeta)\rangle \in \mathcal{H}$ ($k=1$) and a Gaussian state $|\xi,\omega\rangle \in \mathcal{H}$. Recall from the definition of PVGS in (13) that $|\xi,\omega\rangle = |\psi_{\overline{s|}}^{(0)}(\xi,\omega)\rangle$. The inner product $\langle \omega, \xi|\psi_{\overline{t|}}^{(1)}(\mu,\zeta)\rangle$ can be evaluated using (15) with $(h,k) = (0,1)$. By introducing

$$\Psi(\xi,\mu,\omega,\zeta) \triangleq \frac{\eta(\mu,\zeta) - \eta(\xi,\omega)^*\rho(\omega,\zeta)}{\sqrt{1-\rho(\omega,\zeta)^2}}, \quad (17a)$$

$$\Phi(\xi,\mu,\omega,\zeta) \triangleq \frac{\eta(\xi,\omega)^* - \eta(\mu,\zeta)\rho(\omega,\zeta)}{\sqrt{1-\rho(\omega,\zeta)^2}}, \quad (17b)$$

with $(\xi,\mu,\omega,\zeta) \in \mathbb{C}^2 \times \mathbb{C}_*^2$, the orthogonalization condition $\langle\omega,\xi|\psi_{\overline{t|}}^{(1)}(\mu,\zeta)\rangle = 0$ requires satisfying

$$\Psi(\xi,\mu,\omega,\zeta) = 0 \quad \text{for } t = -1, \quad (18a)$$

$$\Phi(\xi,\mu,\omega,\zeta) = 0 \quad \text{for } t = +1, \quad (18b)$$

where, for $(h,k) = (0,1)$, Eq. (18a) follows from (15b) or (15d) and Eq. (18b) follows from (15a) or (15c). Without providing a detailed study of (18), whose generalization will be deeply investigated later, it is worth noticing that both (18a) and (18b) admit infinite solutions. For instance, the subset of solutions $\{(0,0,\omega,\zeta)\}_{(\omega,\zeta)\in\mathbb{C}_*^2}$ contains 4-tuples of parameters that satisfy both (18a) and (18b), meaning that the corresponding set of single-PVGSs $\{|\psi_{\overline{t|}}^{(1)}(0,\zeta)\rangle = \Omega(t,1,0,\zeta)\}_{\zeta\in\mathbb{C}_*} \subseteq \mathcal{H}$ is orthogonal to the set of Gaussian squeezed states $\{|0,\omega\rangle = \Omega(s,0,0,\omega)\}_{\omega\in\mathbb{C}_*} \subseteq \mathcal{H}$.

B. General orthogonalization problem

The following theorem establishes the existence of orthogonal PVGSs.

Theorem 1 (existence of orthogonal PVGSs). Let $h,k \in \mathbb{N}$ with $h \leqslant k$. Then, there exists $(\xi,\mu,\omega,\zeta) \in \mathbb{C}^2 \times \mathbb{C}_*^2$ such that two PVGSs $|\psi_{\overline{s|}}^{(h)}(\xi,\omega)\rangle = \Omega(s,h,\xi,\omega) \in \mathcal{H}$ and $|\psi_{\overline{t|}}^{(k)}(\mu,\zeta)\rangle = \Omega(t,k,\mu,\zeta) \in \mathcal{H}$ are orthogonal. □

Proof. Observe that (15a) and (15d) as well as (15b) and (15c) pairwise exhibit a similar structure. This suggests considering two cases separately, with $s = t$ and $s \neq t$, respectively.

(i) Case with $s = t$. In such a case, the orthogonalization problem involves two PVGSs of the same type, namely two PAGSs when $(s,t) = (+1,+1)$ and two PSGSs when $(s,t) = (-1,-1)$. From (11), note that $|\rho(\omega,\zeta)| \in (0,1)$ for all $(\omega,\zeta) \in \mathbb{C}_*^2$. Therefore, the orthogonalization condition $\langle\psi_{\overline{s|}}^{(h)}(\xi,\omega)|\psi_{\overline{s|}}^{(k)}(\mu,\zeta)\rangle = 0$ requires, respectively from (15a) and (15d), satisfying

$$G_{h,k}(\eta(\xi,\omega)^*, \eta(\mu,\zeta)|\rho(\omega,\zeta), \rho(\omega,\zeta)) = 0 \quad \text{for } s = -1, \quad (19a)$$

$$G_{k,h}(\eta(\xi,\omega)^*, \eta(\mu,\zeta)|\rho(\omega,\zeta), \rho(\omega,\zeta)^{-1}) = 0 \quad \text{for } s = +1. \quad (19b)$$

From (6), the condition (19) can be rewritten as

$$H_{h,k}(2\Phi(\xi,\mu,\omega,\zeta), -1; 2\Psi(\xi,\mu,\omega,\zeta), -1|2\rho(\omega,\zeta)) = 0 \quad \text{for } s = -1, \quad (20a)$$

$$H_{k,h}(2\Phi(\xi,\mu,\omega,\zeta), -1; 2\Psi(\xi,\mu,\omega,\zeta), -1|2\rho(\omega,\zeta)^{-1}) = 0 \quad \text{for } s = +1. \quad (20b)$$

By exploiting the definition of hypergeometric bivariate Hermite polynomials in (3), the conditions (20a) and (20b) can be jointly written as the single condition

$$\mathscr{H}_{h,k}(\eta(\xi,\omega)^*, \eta(\mu,\zeta)|\boldsymbol{\Theta}^{\overline{s|}}(\omega,\zeta)) = 0, \quad (21)$$

where $\boldsymbol{\Theta}^{\overline{s|}}(\omega,\zeta)$ is a symmetric complex matrix given by

$$\boldsymbol{\Theta}^{\overline{s|}}(\omega,\zeta) \triangleq \begin{bmatrix} \frac{2\rho(\omega,\zeta)^{s+1}}{1-\rho(\omega,\zeta)^2} & -\frac{2\rho(\omega,\zeta)}{1-\rho(\omega,\zeta)^2} \\ -\frac{2\rho(\omega,\zeta)}{1-\rho(\omega,\zeta)^2} & \frac{2\rho(\omega,\zeta)^{s+1}}{1-\rho(\omega,\zeta)^2} \end{bmatrix}. \quad (22)$$

Therefore, proving the existence of two orthogonal PVGSs of the same type is equivalent to proving that the algebraic variety

$$\mathscr{Z}_{h,k}^{\overline{s|}} \triangleq \{(\xi,\mu,\omega,\zeta) \in \mathbb{C}^2 \times \mathbb{C}_*^2 : \mathscr{H}_{h,k}(\eta(\xi,\omega)^*, \eta(\mu,\zeta)|\boldsymbol{\Theta}^{\overline{s|}}(\omega,\zeta)) = 0\} \quad (23)$$

is nonempty, i.e., $\mathscr{Z}_{h,k}^{\overline{s|}} \neq \varnothing$. To simplify the problem, define the nonsingular affine transformation

$$\begin{bmatrix} \sigma(\xi,\mu,\omega,\zeta) \\ \delta(\xi,\mu,\omega,\zeta) \end{bmatrix} \triangleq \frac{\boldsymbol{\Theta}^{\overline{s|}}(\omega,\zeta)}{\sqrt{[\boldsymbol{\Theta}^{\overline{s|}}(\omega,\zeta)]_{22}}} \begin{bmatrix} \eta(\xi,\omega)^* \\ \eta(\mu,\zeta) \end{bmatrix}, \quad (24)$$

from which it follows that (23) can be written as

$$\mathscr{Z}_{h,k}^{\overline{s|}} = \{(\xi,\mu,\omega,\zeta) \in \mathbb{C}^2 \times \mathbb{C}_*^2 : \breve{\mathscr{H}}_{h,k}(\sigma(\xi,\mu,\omega,\zeta), \delta(\xi,\mu,\omega,\zeta)|\boldsymbol{\Theta}^{\overline{s|}}(\omega,\zeta)) = 0\}. \quad (25)$$

In particular, Eq. (25) shows that the algebraic variety $\mathscr{Z}_{h,k}^{\overline{s|}}$ is related to the roots of affine hypergeometric bivariate Hermite polynomials obtained through the transformation (24). Now observe that the expansion of such polynomials (given by (4)) is shaped by the matrix $\boldsymbol{\Theta}^{\overline{s|}}(\omega,\zeta)$, which depends on the squeezing parameters of the two PVGSs. To cope with this difficulty, consider an arbitrary pair of squeezing parameters $(\omega,\zeta) = (\omega_0,\zeta_0) \in \mathbb{C}_*^2$ and define

$$\breve{\mathscr{Z}}_{h,k}^{\overline{s|},(\omega_0,\zeta_0)} \triangleq \{(x,y) \in \mathbb{C}^2 : \breve{\mathscr{H}}_{h,k}(x,y|\boldsymbol{\Theta}^{\overline{s|}}(\omega_0,\zeta_0)) = 0\}, \quad (26)$$

which is the nonempty affine algebraic variety of $\breve{\mathscr{H}}_{h,k}(x,y|\boldsymbol{\Theta}^{\overline{s|}}(\omega_0,\zeta_0))$ and an algebraic subvariety of the whole affine one $\breve{\mathscr{Z}}_{h,k}^{\overline{s|}} = \bigcup_{(\omega_0,\zeta_0)\in\mathbb{C}_*^2} \breve{\mathscr{Z}}_{h,k}^{\overline{s|},(\omega_0,\zeta_0)}$. By using (26), define the algebraic (ω_0,ζ_0)-subvariety

$$\mathscr{Z}_{h,k}^{\overline{s|},(\omega_0,\zeta_0)} \triangleq \{(\xi,\mu,\omega_0,\zeta_0) \in \mathbb{C}^2 \times \mathbb{C}_*^2 : \breve{\mathscr{H}}_{h,k}(\sigma(\xi,\mu,\omega_0,\zeta_0), \delta(\xi,\mu,\omega_0,\zeta_0)|\boldsymbol{\Theta}^{\overline{s|}}(\omega_0,\zeta_0)) = 0\}, \quad (27)$$

[4]In Sec. IV we will show that such a condition can be fulfilled.

which contains 4-tuples of parameters that make two PVGSs with fixed squeezing parameters ω_0 and ζ_0, respectively, orthogonal. Substituting (24) into (27) leads to

$$\mathcal{Z}_{h,k}^{\overline{s}\rceil,(\omega_0,\zeta_0)} = \Bigg\{(\xi,\mu,\omega_0,\zeta_0) \in \mathbb{C}^2\times\mathbb{C}_*^2 : \frac{\boldsymbol{\Theta}^{\overline{s}\rceil}(\omega_0,\zeta_0)}{\sqrt{[\boldsymbol{\Theta}^{\overline{s}\rceil}(\omega_0,\zeta_0)]_{22}}}\begin{bmatrix}\eta(\xi,\omega_0)^*\\ \eta(\mu,\zeta_0)\end{bmatrix} = \begin{bmatrix}x\\ y\end{bmatrix}\Bigg\}_{(x,y)\in\breve{\mathcal{Z}}_{h,k}^{\overline{s}\rceil,(\omega_0,\zeta_0)}}, \tag{28}$$

where recall that $\breve{\mathcal{Z}}_{h,k}^{\overline{s}\rceil,(\omega_0,\zeta_0)} \neq \varnothing$. Observe that the whole algebraic variety $\mathcal{Z}_{h,k}^{\overline{s}\rceil}$ can be written as

$$\mathcal{Z}_{h,k}^{\overline{s}\rceil} = \bigcup_{(\omega_0,\zeta_0)\in\mathbb{C}_*^2} \mathcal{Z}_{h,k}^{\overline{s}\rceil,(\omega_0,\zeta_0)}. \tag{29}$$

Therefore, $\mathcal{Z}_{h,k}^{\overline{s}\rceil} \neq \varnothing$ if at least one of its algebraic subvarieties is nonempty. Without loss of generality, consider the (ω_0,ζ_0)-subvariety $\mathcal{Z}_{h,k}^{\overline{s}\rceil,(\omega_0,\zeta_0)}$, which is nonempty if there exists $(\xi,\mu)\in\mathbb{C}^2$ satisfying, with respect to $\eta(\xi,\omega_0)^*$ and $\eta(\mu,\zeta_0)$, one of the systems of linear equations in (28) with constant terms given by the roots of $\mathscr{H}_{h,k}(x,y|\boldsymbol{\Theta}^{\overline{s}\rceil}(\omega_0,\zeta_0))$.

Finally, observe that such a condition is always fulfilled since for $z_0\in\mathbb{C}_*$ it follows that $\mathrm{Dom}(\eta(\cdot,z_0))=\mathbb{C}$, $\mathrm{Ran}(\eta(\cdot,z_0))=\mathbb{C}$ (see Lemma A1 in Appendix A), and

$$\det\left\{\boldsymbol{\Theta}^{\overline{s}\rceil}(\omega_0,\zeta_0)/\sqrt{[\boldsymbol{\Theta}^{\overline{s}\rceil}(\omega_0,\zeta_0)]_{22}}\right\} = -2s \neq 0.$$

Furthermore, since (ω_0,ζ_0) is arbitrary, all algebraic subvarieties given by (28) with different squeezing parameters are nonempty. This proves the existence of orthogonal PVGSs of the same type.

(ii) Case with $s\neq t$. In such a case, the orthogonalization problem involves two PVGSs of different type, namely, a PAGS and a PSGS. The pair (s,t) specifies the order to compute their inner product. Since $|\rho(\omega,\zeta)|\in(0,1)$ for all $(\omega,\zeta)\in\mathbb{C}_*^2$, the orthogonalization conditions $\langle\psi_+^{(h)}(\xi,\omega)|\psi_-^{(k)}(\mu,\zeta)\rangle=0$ and $\langle\psi_-^{(h)}(\xi,\omega)|\psi_+^{(k)}(\mu,\zeta)\rangle=0$ require, from (15b) and (15c), respectively, satisfying

$$G_{0,h+k}(\eta(\xi,\omega)^*,\eta(\mu,\zeta)|\rho(\omega,\zeta),\rho(\omega,\zeta))=0 \quad \text{for } (s,t)=(+1,-1), \tag{30a}$$

$$G_{h+k,0}(\eta(\xi,\omega)^*,\eta(\mu,\zeta)|\rho(\omega,\zeta),\rho(\omega,\zeta))=0 \quad \text{for } (s,t)=(-1,+1). \tag{30b}$$

From (6), Eq. (30) is equivalent to

$$H_{0,h+k}(2\Phi(\xi,\mu,\omega,\zeta),-1;2\Psi(\xi,\mu,\omega,\zeta),-1|2\rho(\omega,\zeta))=0 \quad \text{for } (s,t)=(+1,-1),$$

$$H_{h+k,0}(2\Phi(\xi,\mu,\omega,\zeta),-1;2\Psi(\xi,\mu,\omega,\zeta),-1|2\rho(\omega,\zeta))=0 \quad \text{for } (s,t)=(-1,+1),$$

which from (5), (2), (1), and $H_n(x)=H_n(2x,-1)$ can be further simplified to

$$H_{h+k}(\Psi(\xi,\mu,\omega,\zeta))=0 \quad \text{for } (s,t)=(+1,-1), \tag{31a}$$

$$H_{h+k}(\Phi(\xi,\mu,\omega,\zeta))=0 \quad \text{for } (s,t)=(-1,+1). \tag{31b}$$

Therefore, proving that there exist a PAGS and a PSGS that are orthogonal is equivalent to proving that the algebraic varieties

$$\mathcal{Z}_{0,h+k}^{+,-} \triangleq \{(\xi,\mu,\omega,\zeta)\in\mathbb{C}^2\times\mathbb{C}_*^2 : H_{h+k}(\Psi(\xi,\mu,\omega,\zeta))=0\} \quad \text{for } (s,t)=(+1,-1), \tag{32a}$$

$$\mathcal{Z}_{h+k,0}^{-,+} \triangleq \{(\xi,\mu,\omega,\zeta)\in\mathbb{C}^2\times\mathbb{C}_*^2 : H_{h+k}(\Phi(\xi,\mu,\omega,\zeta))=0\} \quad \text{for } (s,t)=(-1,+1) \tag{32b}$$

are nonempty, i.e., $\mathcal{Z}_{0,h+k}^{+,-}\neq\varnothing$ and $\mathcal{Z}_{h+k,0}^{-,+}\neq\varnothing$. Recall that the algebraic variety of the single-variable Hermite polynomial $H_{h+k}(x)$ is the finite set of real points

$$\mathcal{Z}_{h+k} \triangleq \{x\in\mathbb{R} : H_{h+k}(x)=0\}, \tag{33}$$

with cardinality $|\mathcal{Z}_{h+k}|=h+k$. Thus, $\mathcal{Z}_{0,h+k}^{+,-}$ and $\mathcal{Z}_{h+k,0}^{-,+}$ in (32) can be written as

$$\mathcal{Z}_{0,h+k}^{+,-} = \{(\xi,\mu,\omega,\zeta)\in\mathbb{C}^2\times\mathbb{C}_*^2 : \Psi(\xi,\mu,\omega,\zeta)=x\}_{x\in\mathcal{Z}_{h+k}} \quad \text{for } (s,t)=(+1,-1), \tag{34a}$$

$$\mathcal{Z}_{h+k,0}^{-,+} = \{(\xi,\mu,\omega,\zeta)\in\mathbb{C}^2\times\mathbb{C}_*^2 : \Phi(\xi,\mu,\omega,\zeta)=x\}_{x\in\mathcal{Z}_{h+k}} \quad \text{for } (s,t)=(-1,+1) \tag{34b}$$

and are nonempty if at least one of the $h+k$ equations $\{\Psi(\xi,\mu,\omega,\zeta)=x\}_{x\in\mathcal{Z}_{h+k}}$, for $(s,t)=(+1,-1)$, and $\{\Phi(\xi,\mu,\omega,\zeta)=x\}_{x\in\mathcal{Z}_{h+k}}$, for $(s,t)=(-1,+1)$, has solutions. Finally, by observing that $\mathrm{Dom}(\Psi)=\mathrm{Dom}(\Phi)=\mathbb{C}^2\times\mathbb{C}_*^2$ and $\mathrm{Ran}(\Psi)\cap\mathrm{Ran}(\Phi)\supseteq\mathbb{R}$ (see Lemma B1 in Appendix B), it follows that both $\mathcal{Z}_{0,h+k}^{+,-}$ $\mathcal{Z}_{h+k,0}^{-,+}$ are nonempty. This proves the existence of orthogonal PVGSs of different type. ⊠

Remark 2. Theorem 1 provides an algebraic interpretation of why Gaussian states are always nonorthogonal. Consider two Gaussian states $|\xi,\omega\rangle, |\mu,\zeta\rangle\in\mathcal{H}$. From the definition of PVGS in (13), we have that $|\xi,\omega\rangle=|\psi_{\overline{s}\rceil}^{(0)}(\xi,\omega)\rangle$ and $|\mu,\zeta\rangle=|\psi_{\overline{t}\rceil}^{(0)}(\mu,\zeta)\rangle$. Therefore, the inner product between the two Gaussian states can be evaluated using the expressions for the inner product between two PVGSs with $(h,k)=(0,0)$ as

$$\langle\omega,\xi|\mu,\zeta\rangle = \langle\psi_{\overline{s}\rceil}^{(0)}(\xi,\omega)|\psi_{\overline{t}\rceil}^{(0)}(\mu,\zeta)\rangle.$$

Now consider the cases with $s=t$ and $s\neq t$ separately. When $s=t$, it follows from (26) that for all $(\omega_0,\zeta_0)\in\mathbb{C}_*^2$, $\breve{\mathcal{Z}}_{h,k}^{\overline{s}\rceil,(\omega_0,\zeta_0)}=\varnothing$ as $\mathscr{H}_{0,0}(x,y|\boldsymbol{\Theta}^{\overline{s}\rceil}(\omega_0,\zeta_0))=1$. Using this fact in (28) and (29) leads to $\mathcal{Z}_{0,0}^{\overline{s}\rceil}=\varnothing$. When $s\neq t$, Eq. (33) shows that $\mathcal{Z}_0=\varnothing$ as $H_0(x)=1$. Then $\mathcal{Z}_{0,0}^{+,-}=\varnothing=\mathcal{Z}_{0,0}^{-,+}$ easily follows from (34). □

IV. DESIGN METHODOLOGIES FOR ORTHOGONAL PVGSS

This section studies the geometrical properties of the algebraic varieties associated with the inner product between PVGSs, derives mathematical relations between physical parameters for implementing distinguishable PVGSs, and develops low-complexity algorithms to determine such parameters using standard programming platforms.

ALGORITHM 1. Orthogonal PVGSs of the same type.

1: **Input**: Type of PVGSs s, number of photon-variation operations $(h,k)\in\mathbb{N}^2$ with $h\leqslant k$, squeezing parameters $(\omega_0,\zeta_0)\in\mathbb{C}^2_*$
2: Compute $\boldsymbol{\Theta}^{\overline{s}|}(\omega_0,\zeta_0)$ using (22) and calculate $\breve{\mathcal{Z}}^{\overline{s}|,(\omega_0,\zeta_0)}_{h,k}$ employing (26)
3: Choose a root $(x,y)\in\breve{\mathcal{Z}}^{\overline{s}|,(\omega_0,\zeta_0)}_{h,k}$ and solve the $(\omega_0,\zeta_0,(x,y))$-system of equations (36) with respect to $\eta(\xi,\omega_0)^*$ and $\eta(\mu,\zeta_0)$
4: Use (10) to determine displacement parameters (ξ_0,μ_0)
5: **Output**: 4-tuple of parameters $(\xi_0,\mu_0,\omega_0,\zeta_0)\in\mathcal{Z}^{\overline{s}|,(\omega_0,\zeta_0)}_{h,k}$ that make the PVGSs orthogonal

A. Design of orthogonal PVGSs of the same type

When $s=t$, the orthogonalization problem involves two PVGSs of the same type. From (29), the whole algebraic variety $\mathcal{Z}^{\overline{s}|}_{h,k}$ is obtained as the union of its algebraic subvarieties and exhibits a complex structure that challenges the study of its geometrical properties. To cope with this, let us focus on the subvarieties separately. Without loss of generality, consider the (ω_0,ζ_0)-subvariety $\mathcal{Z}^{\overline{s}|,(\omega_0,\zeta_0)}_{h,k}$, which contains all the 4-tuples $(\xi,\mu,\omega_0,\zeta_0)\in\mathbb{C}^2\times\mathbb{C}^2_*$, with (ξ,μ) satisfying the corresponding set of equations

$$\left\{\frac{\boldsymbol{\Theta}^{\overline{s}|}(\omega_0,\zeta_0)}{\sqrt{[\boldsymbol{\Theta}^{\overline{s}|}(\omega_0,\zeta_0)]_{22}}}\begin{bmatrix}\eta(\xi,\omega_0)^*\\ \eta(\mu,\zeta_0)\end{bmatrix}=\begin{bmatrix}x\\ y\end{bmatrix}\right\}_{(x,y)\in\breve{\mathcal{Z}}^{\overline{s}|,(\omega_0,\zeta_0)}_{h,k}}. \tag{35}$$

Recall that $\breve{\mathcal{Z}}^{\overline{s}|,(\omega_0,\zeta_0)}_{h,k}$ is the affine algebraic subvariety of $\mathscr{H}_{h,k}(x,y|\boldsymbol{\Theta}^{\overline{s}|}(\omega_0,\zeta_0))$. Notice that $\breve{\mathcal{Z}}^{\overline{s}|,(\omega_0,\zeta_0)}_{h,k}$ contains infinite roots that parametrize the systems of equations in (35). For $(x,y)\in\breve{\mathcal{Z}}^{\overline{s}|,(\omega_0,\zeta_0)}_{h,k}$, the corresponding $(\omega_0,\zeta_0,(x,y))$-system can be easily solved with respect to $\eta(\xi,\omega_0)^*$ and $\eta(\mu,\zeta_0)$ using Cramer's rule, which leads to

$$\begin{aligned}\eta(\xi,\omega_0)^*&=-s\frac{\rho(\omega_0,\zeta_0)}{1-\rho(\omega_0,\zeta_0)^2}\sqrt{\frac{1-\rho(\omega_0,\zeta_0)^2}{2\rho(\omega_0,\zeta_0)^{s+1}}}\\&\quad\times\ (x\rho(\omega_0,\zeta_0)^s+y),\\ \eta(\mu,\zeta_0)&=-s\frac{\rho(\omega_0,\zeta_0)}{1-\rho(\omega_0,\zeta_0)^2}\sqrt{\frac{1-\rho(\omega_0,\zeta_0)^2}{2\rho(\omega_0,\zeta_0)^{s+1}}}\\&\quad\times\ (x+y\rho(\omega_0,\zeta_0)^s).\end{aligned} \tag{36}$$

Equations (10), (35), and (36) are pivotal to designing orthogonal PVGSs of the same type. Indeed, their combined use allows one to determine the parameters making PVGSs orthogonal via the methodology presented in Algorithm 1. In particular, given the type, the number of photon-variation operations, and a pair of squeezing parameters as input (step 1), Algorithm 1 computes pairs of displacement parameters (steps 2, 3, and 4) and returns 4-tuples of parameters that make two PVGSs of the same type orthogonal (step 5).

Remark 3. A single-variable Hermite polynomial $H_n(x)$ with odd degree has one root at $x=0$. From (4), it follows that when $h+k$ is odd, $\mathscr{H}_{h,k}(0,0|\boldsymbol{\Theta}^{\overline{s}|}(\omega_0,\zeta_0))=0$, and thus $(0,0)\in\breve{\mathcal{Z}}^{\overline{s}|,(\omega_0,\zeta_0)}_{h,k}$. By using (10), $(\mu,\xi)=(0,0)$ satisfies (36) with $(x,y)=(0,0)$. Since (ω_0,ζ_0) is arbitrary, we find that when $h+k$ is odd, two PVGSs of the same type $|\psi^{(h)}_{\overline{s}|}(0,\omega)\rangle$ and $|\psi^{(k)}_{\overline{s}|}(0,\zeta)\rangle$ are always orthogonal independently of their squeezing parameters. □

Since the algebraic subvariety $\mathcal{Z}^{\overline{s}|,(\omega_0,\zeta_0)}_{h,k}$ is a set of complex 4-tuples, visualizing its geometrical structure is difficult. Nonetheless, in simple settings, the structure of $\mathcal{Z}^{\overline{s}|,(\omega_0,\zeta_0)}_{h,k}$ can be represented, thus facilitating the establishment of design methodologies for orthogonal PVGSs. Consider $(\omega_0,\zeta_0)\in\mathbb{R}^2_-$, leading to $\rho(\omega_0,\zeta_0)\in(0,1)$, and $(x,y)\in\breve{\mathcal{Z}}^{\overline{s}|,(\omega_0,\zeta_0)}_{h,k}\cap\mathbb{R}^2$. In these settings, the $(\omega_0,\zeta_0,(x,y))$-system in (36) simplifies to

$$\begin{aligned}\eta(\xi,\omega_0)^*&=-s\sqrt{\frac{\rho(\omega_0,\zeta_0)^{1-s}}{2(1-\rho(\omega_0,\zeta_0)^2)}}(x\rho(\omega_0,\zeta_0)^s+y),\\ \eta(\mu,\zeta_0)&=-s\sqrt{\frac{\rho(\omega_0,\zeta_0)^{1-s}}{2(1-\rho(\omega_0,\zeta_0)^2)}}(x+y\rho(\omega_0,\zeta_0)^s).\end{aligned} \tag{37}$$

Since the right-hand side in (37) is real, using (10) in the left-hand side leads to $(\xi,\mu)\in\mathbb{R}^2$. After some algebra, it can be found that

$$\begin{aligned}\xi&=-s\sqrt{\frac{\tanh(|\omega_0|)\rho(\omega_0,\zeta_0)^{1-s}}{1-\rho(\omega_0,\zeta_0)^2}}\frac{x\rho(\omega_0,\zeta_0)^s+y}{1+\tanh(|\omega_0|)},\\ \mu&=-s\sqrt{\frac{\tanh(|\zeta_0|)\rho(\omega_0,\zeta_0)^{1-s}}{1-\rho(\omega_0,\zeta_0)^2}}\frac{x+y\rho(\omega_0,\zeta_0)^s}{1+\tanh(|\zeta_0|)}.\end{aligned} \tag{38}$$

Then, by varying $(x,y)\in\breve{\mathcal{Z}}^{\overline{s}|,(\omega_0,\zeta_0)}_{h,k}\cap\mathbb{R}^2$, the subvariety $\mathcal{Z}^{\overline{s}|,(\omega_0,\zeta_0)}_{h,k}\subseteq\mathbb{R}^2\times\mathbb{R}^2_-$ contains real 4-tuples having the same real squeezing parameters. Therefore, the geometrical structure of $\mathcal{Z}^{\overline{s}|,(\omega_0,\zeta_0)}_{h,k}$ varies only along real algebraic curves $\{(\xi,\mu)\}_{(x,y)\in\breve{\mathcal{Z}}^{\overline{s}|,(\omega_0,\zeta_0)}_{h,k}\cap\mathbb{R}^2}$, whose points are the pairs of displacement parameters given by (38).

Figure 2 represents the inner product between two PAGSs and the corresponding algebraic curves for displacement parameters that make such states orthogonal, where $h=2$, $k=3$, and $(\omega_0,\zeta_0)=(-0.8,-0.5)$. With these settings, the inner product is real and it is depicted by Fig. 2(a), where red solid curves are the algebraic curves, computed numerically, along which the displacement parameters make the inner product zero. Figure 2(b) displays the real subvariety $\mathcal{Z}^{+,(\omega_0,\zeta_0)}_{h,k}$ projected on the $\xi\mu$ plane and consisting of curves with equations given by (38), with $s=+1$. Note that such curves match the ones computed numerically and shown in Fig. 2(a).

Likewise, Fig. 3 illustrates the inner product between two PSGSs and the algebraic curves for displacement parameters using $h=2$, $k=2$, and $(\omega_0,\zeta_0)=(-0.8,-0.2)$. Also in this scenario, despite the more irregular surface of the inner product, the numerical algebraic curves for displacement parameters in Fig. 3(a) are matched by the curves described by (38), with $s=-1$, and represented in Fig. 3(b).

B. Design of orthogonal PVGSs of different type

When $s\neq t$, the pair (s,t) specifies the order to compute the inner product between a PSGS and a PAGS. From (32), the algebraic varieties $\mathcal{Z}^{+,-}_{0,h+k}$ and $\mathcal{Z}^{-,+}_{h+k,0}$ contain 4-tuples

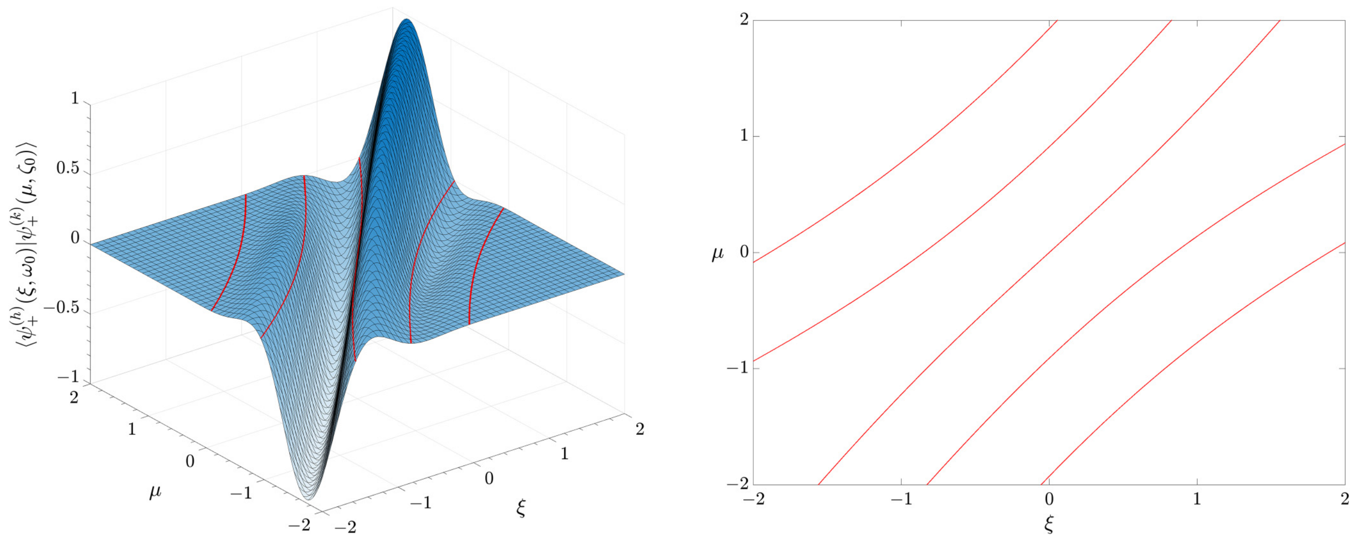

(a) (b)

FIG. 2. Representation of (a) the inner product between two PAGSs with algebraic curves (red solid curves) for displacement parameters computed numerically and (b) algebraic curves for displacement parameters obtained by projecting the algebraic subvariety $\mathcal{Z}_{h,k}^{+,(\omega_0,\zeta_0)}$ on the $\xi\mu$ plane and given by (38) with $s = +1$. Results are obtained by setting $h = 2$, $k = 3$, and $(\omega_0, \zeta_0) = (-0.8, -0.5)$.

of parameters belonging to sets of $h+k$ hypersurfaces with equations

$$\{\Psi(\xi,\mu,\omega,\zeta) = x\}_{x\in\mathcal{Z}_{h+k}} \quad \text{for } (s,t) = (+1,-1), \tag{39a}$$

$$\{\Phi(\xi,\mu,\omega,\zeta) = x\}_{x\in\mathcal{Z}_{h+k}} \quad \text{for } (s,t) = (-1,+1) \tag{39b}$$

and parametrized by the roots of a single-variable Hermite polynomial with degree $h+k$. Equations (10), (17), and (39) can be used to establish the parameters making PVGSs orthogonal. Algorithm 2 presents the methodology for designing orthogonal PVGSs of the same type. Given the type of PVGSs and the number of photon-variation operations as input (step 1), Algorithm 2 computes 4-tuples of parameters that make the PVGSs orthogonal (steps 2 and 3) and finally returns them (step 4).

Remark 4. Recall that when $h+k$ is odd, $0 \in \mathcal{Z}_{h+k}$ and the corresponding equations $\Psi(\xi,\mu,\omega,\zeta) = 0$ for $(s,t) = (+1,-1)$ and $\Phi(\xi,\mu,\omega,\zeta) = 0$ for $(s,t) = (-1,+1)$ admit solutions having the form $(0,0,\omega,\zeta)$ for all $(\omega,\zeta) \in \mathbb{C}_*^2$. It follows that when $h+k$ is odd, two PVGSs of different type $|\psi_{\overline{s}|}^{(h)}(0,\omega)\rangle$ and $|\psi_{\overline{t}|}^{(k)}(0,\zeta)\rangle$ are always orthogonal independently of their squeezing parameters. □

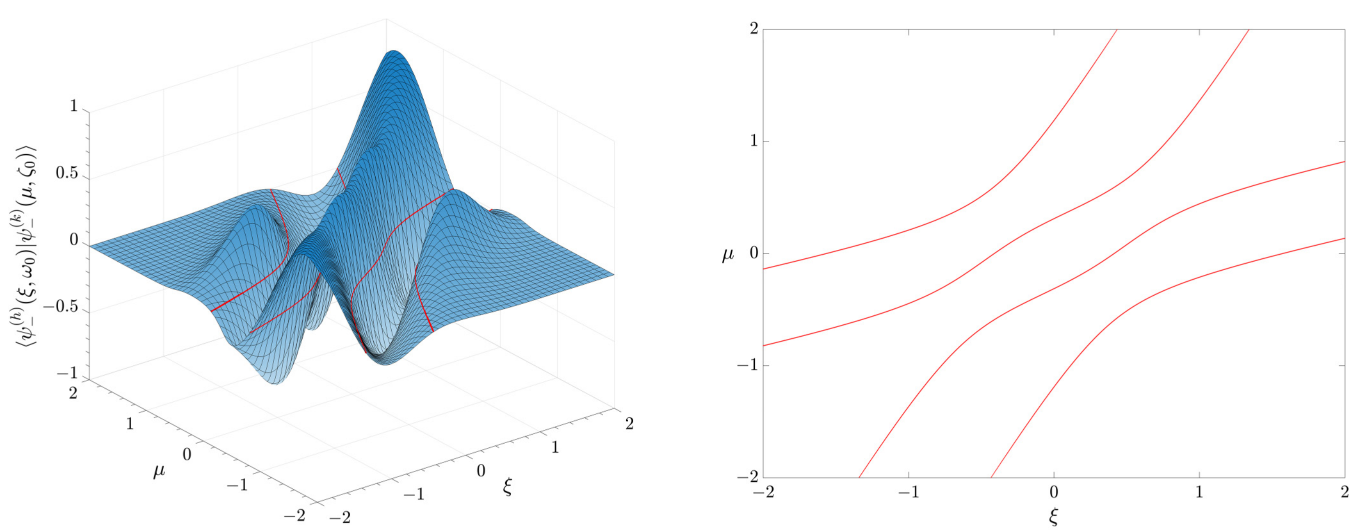

(a) (b)

FIG. 3. Representation of (a) the inner product between two PSGSs with algebraic curves (red solid curves) for displacement parameters computed numerically and (b) algebraic curves for displacement parameters obtained by projecting the algebraic subvariety $\mathcal{Z}_{h,k}^{-,(\omega_0,\zeta_0)}$ on the $\xi\mu$ plane and given by (38) with $s = -1$. Results are obtained by setting $h = 2$, $k = 2$, and $(\omega_0, \zeta_0) = (-0.8, -0.2)$.

ALGORITHM 2. Orthogonal PVGSs of different type.

1: **Input**: Type of PVGSs $(s, t) \in \{(+1, -1), (-1, +1)\}$, number of photon-variation operations $(h, k) \in \mathbb{N}^2$ with $h \leqslant k$
2: Use (33) to find the roots of $H_n(x)$, thus determining the algebraic variety $\mathcal{Z}_{h+k}$
3: Choose a root $x \in \mathcal{Z}_{h+k}$ and solve the corresponding equation in (39), namely, $\Psi(\xi, \mu, \omega, \zeta) = x$ for $(s, t) = (+1, -1)$ and $\Phi(\xi, \mu, \omega, \zeta) = x$ for $(s, t) = (-1, +1)$
4: **Output**: 4-tuple of parameters $(\xi, \mu, \omega, \zeta) \in \mathcal{Z}^{+,-}_{0,h+k}$, for $(s, t) = (+1, -1)$ and $(\xi, \mu, \omega, \zeta) \in \mathcal{Z}^{-,+}_{h+k,0}$, for $(s, t) = (-1, +1)$ that make the PVGSs orthogonal

As for PVGSs of the same type, visualizing the algebraic varieties $\mathcal{Z}^{+,-}_{0,h+k}$ and $\mathcal{Z}^{-,+}_{h+k,0}$ is difficult. Nonetheless, in simple settings it is possible to represent algebraic subvarieties, thus obtaining insights into their geometrical structure and establishing simple orthogonalization methodologies. To do this, first consider $(\omega_0, \zeta_0) \in \mathbb{R}^2_-$, leading to $\rho(\omega_0, \zeta_0) \in (0, 1)$, and pick a root (which is real) $x \in \mathcal{Z}_{h+k}$. From (39), the 4-tuples of parameters that make the PVGSs orthogonal are found by determining all the pairs (ξ, μ) that solve

$$\Psi(\xi, \mu, \omega_0, \zeta_0) = x \quad \text{for } (s, t) = (+1, -1), \tag{40a}$$

$$\Phi(\xi, \mu, \omega_0, \zeta_0) = x \quad \text{for } (s, t) = (-1, +1). \tag{40b}$$

By using (17) and (10) and looking for real solutions to (40a) and (40b), we obtain

$$\mu = \frac{\tanh(|\zeta_0|)[1 + \tanh(|\omega_0|)]}{1 + \tanh(|\zeta_0|)}\xi + x\frac{\sqrt{2\tanh(|\zeta_0|)[1 - \tanh(|\omega_0|)\tanh(|\zeta_0|)]}}{1 + \tanh(|\zeta_0|)} \quad \text{for } (s, t) = (+1, -1), \tag{41a}$$

$$\mu = \frac{1 + \tanh(|\omega_0|)}{\tanh(|\omega_0|)[1 + \tanh(|\zeta_0|)]}\xi - x\frac{\sqrt{2[1 - \tanh(|\omega_0|)\tanh(|\zeta_0|)]}}{\sqrt{\tanh(|\omega_0|)}[1 + \tanh(|\zeta_0|)]} \quad \text{for } (s, t) = (-1, +1), \tag{41b}$$

which describes a straight line with slope and μ intercept depending on ω_0 and ζ_0 and on ω_0, ζ_0, and x, respectively. Since $|\mathcal{Z}_{h+k}| = h + k$, there exist $h + k$ parallel straight lines (one for each root) along which ξ and μ can be chosen to obtain real 4-tuples making the two PVGSs orthogonal.

Figure 4(a) represents the inner product between a PAGS and a PSGS, i.e., $(s, t) = (+1, -1)$, and the corresponding algebraic curves, computed numerically, for displacement parameters that make such states orthogonal, where $h = 3$, $k = 3$, and $(\omega_0, \zeta_0) = (-0.6, -0.4)$. Figure 4(b) shows in the $\xi\mu$ plane the algebraic curves for displacement parameters given by (41a). Notice that such curves match the numerical ones in Fig. 4(a), thus showing that (41a) can be used to design orthogonal PVGSs.

Analogously, Fig. 5 depicts the inner product between a PSGS and a PAGS, i.e., $(s, t) = (-1, +1)$, and the algebraic curves for displacement parameters using $h = 3$, $k = 4$, and $(\omega_0, \zeta_0) = (-0.5, -0.8)$. Also in this scenario, the algebraic curves in the $\xi\mu$ plane displayed by Fig. 5(b) and having analytical expression (41b) overlap the numerical curves shown in Fig. 5(a).

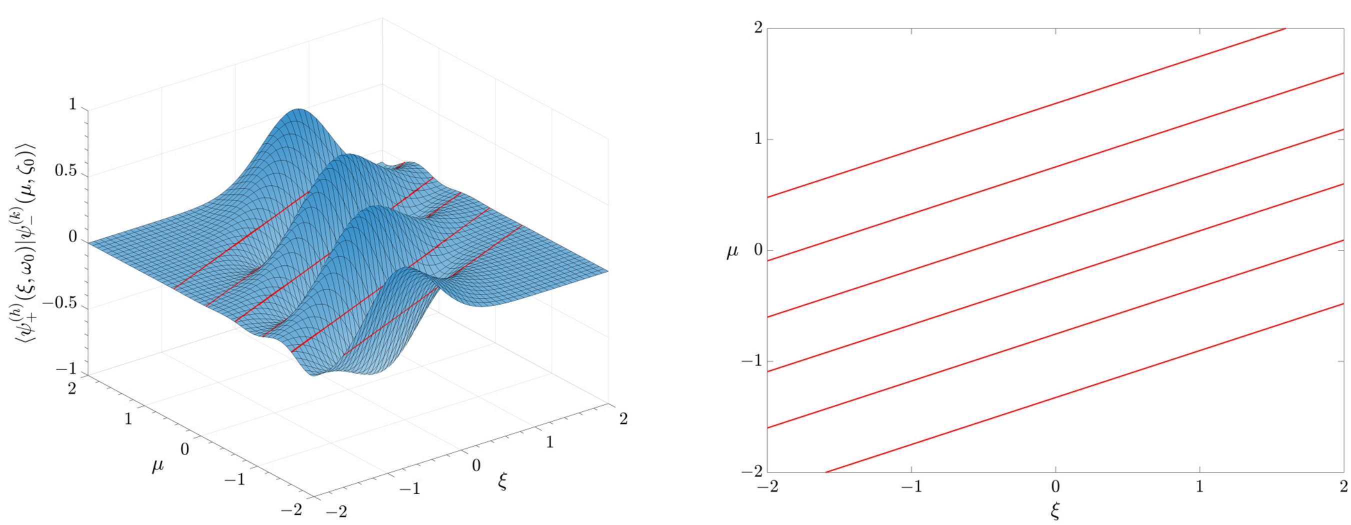

(a) (b)

FIG. 4. Representation of (a) the inner product between a PAGS and a PSGS with algebraic curves (red solid lines) for displacement parameters computed numerically and (b) algebraic curves for displacement parameters on the $\xi\mu$ plane and given by (41a). Results are obtained by setting $h = 3$, $k = 3$, and $(\omega_0, \zeta_0) = (-0.6, -0.4)$.

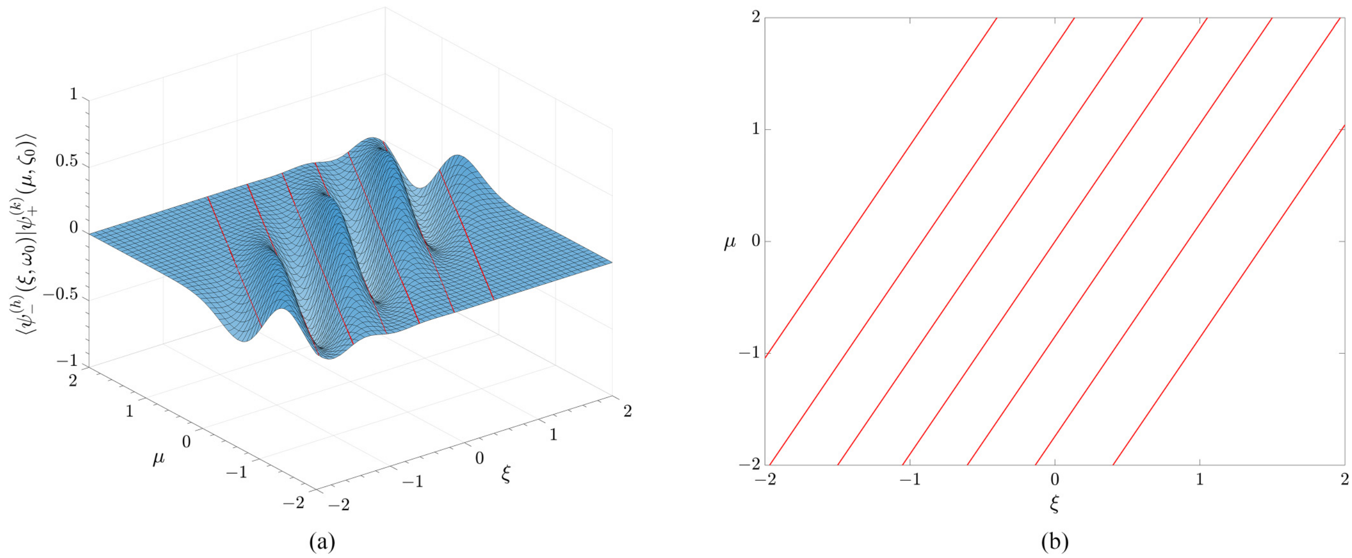

FIG. 5. Representation of (a) the inner product between a PSGS and a PAGS with algebraic curves (red solid lines) for displacement parameters computed numerically and (b) algebraic curves for displacement parameters on the $\xi\mu$ plane and given by (41b). Results are obtained by setting $h = 3$, $k = 4$, and $(\omega_0, \zeta_0) = (-0.5, -0.8)$.

Notice that the algebraic varieties and algebraic curves for displacement parameters associated with the inner product between PVGSs of the same type exhibit a more complex structure than those associated with the inner product between PVGSs of different type. By noting that

$$\langle\psi_{\bar{s}|}^{(h)}(\xi,\omega)|\psi_{\bar{t}|}^{(k)}(\mu,\zeta)\rangle \propto \begin{cases} \langle\omega,\xi|(A^{\dagger})^{h}A^{k}|\mu,\zeta\rangle & \text{for } (s,t)=(-1,-1) \\ \langle\omega,\xi|A^{h}(A^{\dagger})^{k}|\mu,\zeta\rangle & \text{for } (s,t)=(+1,+1) \\ \langle\omega,\xi|A^{h+k}|\mu,\zeta\rangle & \text{for } (s,t)=(+1,-1) \\ \langle\omega,\xi|(A^{\dagger})^{h+k}|\mu,\zeta\rangle & \text{for } (s,t)=(-1,+1) \end{cases}$$

the different complexity can be attributed to the fact that the distinguishability is influenced by the effects of both photon addition and photon subtraction in the former case, whereas it is influenced by only one of these operations in the latter case.

Remark 5. The developed methodologies allow for determining 4-tuples of parameters that make PVGSs distinguishable. While there are no mathematical restrictions on the choice of the 4-tuples yielding orthogonality, different 4-tuples may entail distinct physical implications that must be taken into account in practice, at both the implementation and application levels. From the implementation viewpoint, given the practical difficulty of stably generating large squeezing, choosing 4-tuples with smaller squeezing may be more appropriate. From the application viewpoint, distinct 4-tuples can result in PVGSs with different levels of energy, which is a central resource to be optimized in quantum systems. Furthermore, performance requirements of certain applications may not be stringent enough to require orthogonality between PVGSs. In this situation, one can still use the developed framework by just accounting for an ε tolerance on the distinguishability. □

V. DISTINGUISHABILITY UNDER NOISY QUANTUM DYNAMICS

The findings above unveil the existence of distinguishable PVGSs, thereby potentially allowing for alleviating limitations caused by the nonorthogonality of Gaussian states. This section is devoted to understanding whether, and to what extent, the distinguishability between initial PVGSs can be preserved under noisy time evolution, thus providing insights into quantum state design for practical quantum systems.

A. Distinguishability degradation induced by noise

We first explore whether the distinguishability between PVGSs can be preserved under noisy time evolution. To this aim, it is necessary to utilize the formalism of density operators: let $\mathfrak{D}(\mathcal{H})$ be the set of density operators associated with the Hilbert space $\mathcal{H}$ of the single-mode quantum field.[5]

Definition 2 (quantum distinguishability in $\mathfrak{D}(\mathcal{H})$). Two quantum states $\Xi_1, \Xi_2 \in \mathfrak{D}(\mathcal{H})$ are distinguishable if $\|\Xi_1 - \Xi_2\|_1 = 2$. □

When $\Xi_1, \Xi_2 \in \mathfrak{D}(\mathcal{H})$ are density operators associated with two pure states $|\psi\rangle, |\phi\rangle \in \mathcal{H}$, respectively, then

$$\|\Xi_1 - \Xi_2\|_1 = 2\sqrt{1 - |\langle\psi|\phi\rangle|^2}, \tag{42}$$

which shows the connection between Definitions 1 and 2.

Consider a noisy time evolution of quantum states that obeys the Gorini-Kossakowski-Sudarshan-Lindblad (GKSL) equation [41,42]

$$\frac{d}{dt}\Xi(t) = \mathcal{L}[\Xi(t)] \tag{43a}$$

[5]Hereafter, the terms "quantum state" and "density operator" are used interchangeably.

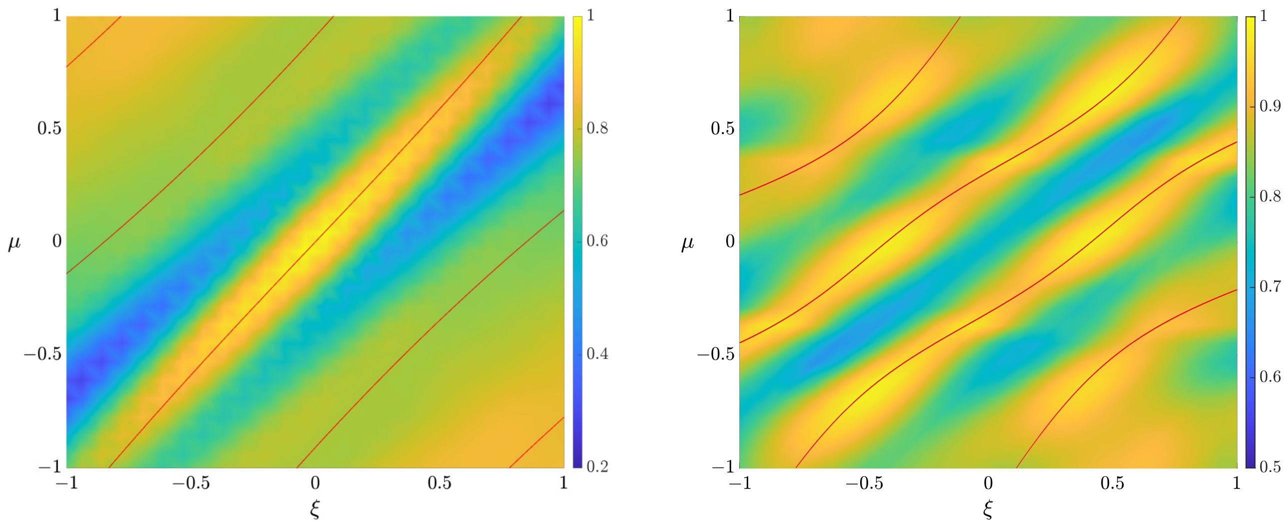

(a) (b)

FIG. 6. Distinguishability between noisy PVGSs of the same type obtained via time evolution in the presence of dephasing with superimposed algebraic curves for displacement parameters given by (38). The decay rate is set to $\kappa = 0.2$ (in units of inverse time), whereas the parameters of the PVGSs are those used in Figs. 2 and 3 for (a) two PAGSs; and (b) two PSGSs, respectively.

$$= -\imath [\![\boldsymbol{H}, \Xi(t)]\!]_- + \sum_k \boldsymbol{L}_k \Xi(t) \boldsymbol{L}_k^\dagger - \frac{1}{2}[\![\boldsymbol{L}_k^\dagger \boldsymbol{L}_k, \Xi(t)]\!]_+, \quad (43b)$$

where $\mathcal{L}$ is the Lindblad superoperator, $\Xi(t)$ is the state of the quantum field at time $t \geqslant 0$, $\boldsymbol{H}$ is the quantum system's Hamiltonian, and $\boldsymbol{L}_k$ denotes the Lindblad (jump) operator associated with the kth noise process.[6] The GKSL equation (43) describes the time evolution of a quantum state in the Markovian regime.[7] For $t \geqslant 0$, the GKSL equation defines, via the Lindblad superoperator (generator) $\mathcal{L}$, a t-parametrized collection of completely positive trace-preserving maps (i.e., quantum channels) $\{\mathcal{E}_t \triangleq e^{t\mathcal{L}}\}_{t\geqslant 0}$, which forms a quantum dynamical semigroup [41]. It follows that $\Xi(t) = \mathcal{E}_t(\Xi(0))$.

To determine the effects of noisy time evolution on the distinguishability between initial PVGSs, we observe that for any pair of initial quantum states $\Xi_1(0)$ and $\Xi_2(0) \in \mathfrak{D}(\mathcal{H})$, the inequality

$$\|\Xi_1(0) - \Xi_2(0)\|_1 \geqslant \|\mathcal{E}_t(\Xi_1(0)) - \mathcal{E}_t(\Xi_2(0))\|_1 \quad (44a)$$
$$= \|\Xi_1(t) - \Xi_2(t)\|_1 \quad (44b)$$

holds for all $t \geqslant 0$ and follows from the fact that the quantum dynamical semigroup $\{\mathcal{E}_t \triangleq e^{t\mathcal{L}}\}_{t\geqslant 0}$ is nonstrictly contractive in the trace-norm $\|\cdot\|_1$. Consequently, noisy states are closer in trace-norm distance than the initial ones, thus yielding distinguishability reduction. Such distinguishability is preserved when the quantum dynamical semigroup generates isometric maps on $\mathfrak{D}(\mathcal{H})$. Equation (44) thus shows that orthogonal PVGSs generally lose their distinguishability during noisy time evolution.

B. Distinguishability under quantum coherence loss

Given that noisy time evolution generally reduces the distinguishability between initially orthogonal PVGSs, we now assess to what extent such distinguishability can be preserved under decoherence. In particular, we consider dephasing, a primary source of noise that arises from random phase fluctuations and causes loss of coherence in quantum systems.[8]

Using the GKSL equation (43), the effect of dephasing on quantum state evolution is described via the single Lindblad jump operator $\boldsymbol{L} = \sqrt{\kappa}\,\boldsymbol{A}^\dagger\boldsymbol{A}$ (the subscript k is omitted for notational simplicity), which leads to the quantum dynamical evolution

$$\frac{d}{dt}\Xi(t) = -\imath [\![\boldsymbol{H}, \Xi(t)]\!]_- + \kappa \boldsymbol{A}^\dagger\boldsymbol{A}\,\Xi(t)\,\boldsymbol{A}^\dagger\boldsymbol{A} - \frac{\kappa}{2}[\![(\boldsymbol{A}^\dagger\boldsymbol{A})^2, \Xi(t)]\!]_+, \quad (45)$$

where κ is the dephasing rate. From Definition 2, the distinguishability between two PVGSs $\Xi_1(t), \Xi_2(t) \in \mathfrak{D}(\mathcal{H})$ evolved under dephasing can be quantified by assessing $\|\Xi_1(t) - \Xi_2(t)\|_1/2$, with $\Xi_1(t)$ and $\Xi_2(t)$ denoting the solutions to (45) with $\Xi_1(0) = |\psi_{\mathfrak{s}]}^{(h)}(\xi,\omega)\rangle\langle\psi_{\mathfrak{s}]}^{(h)}(\xi,\omega)|$ and $\Xi_2(0) = |\psi_{\mathfrak{l}]}^{(k)}(\mu,\zeta)\rangle\langle\psi_{\mathfrak{l}]}^{(k)}(\mu,\zeta)|$, respectively.

[6] In the absence of quantum noise, the GKSL equation reduces to the Liouville–von Neumann equation.

[7] While a more general form of (43) can be defined to account for non-Markovian time evolution, this form describes noise processes that are of interest for practical quantum systems.

[8] Another type of noise in quantum systems is the photon loss generated by the single Lindblad jump operator $\boldsymbol{L} \propto \boldsymbol{A}$. Photon loss causes energy dissipation, unlike dephasing, thereby reducing the distinguishability between quantum states. Dephasing is energy preserving and therefore its effects on the distinguishability between quantum states are less intuitive.

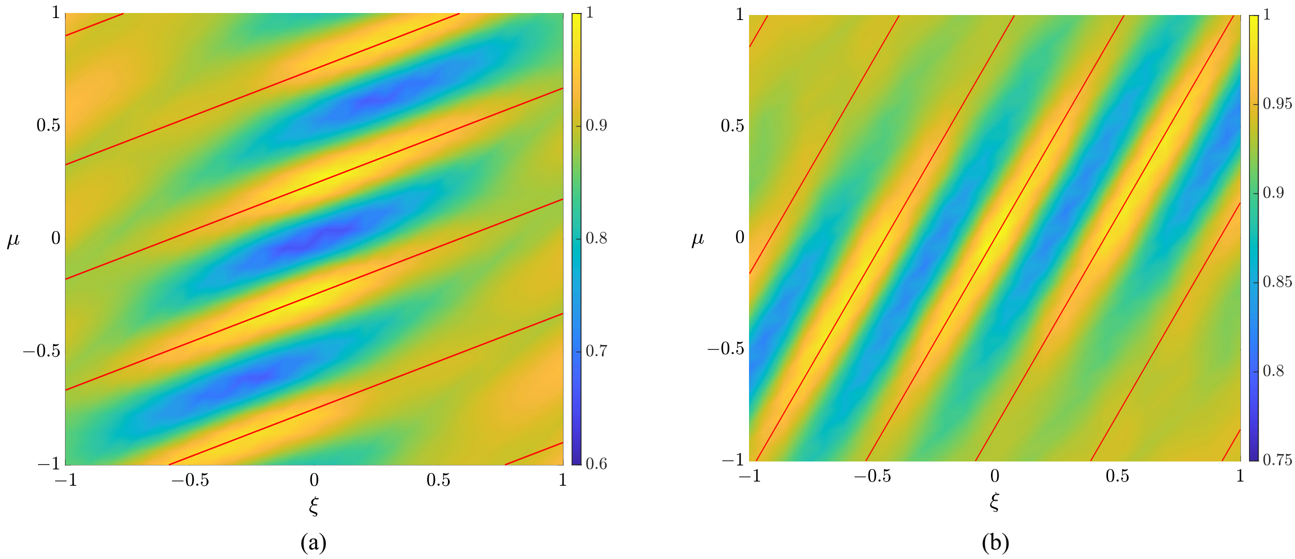

FIG. 7. Distinguishability between noisy PVGSs of different type obtained via time evolution in the presence of dephasing with superimposed algebraic curves for displacement parameters given by (41). The decay rate is set to $\kappa = 0.2$ (in units of inverse time), whereas the parameters of the PVGSs are those used in Figs. 4 and 5 for (a) a PAGS and a PSGS; and (b) a PSGS and a PAGS, respectively.

Figure 6 shows the distinguishability $\|\Xi_1(t) - \Xi_2(t)\|_1/2$ of PVGSs of the same type affected by decoherence due to dephasing and the algebraic curves for the displacement parameters that make the initial PVGSs distinguishable. In particular, Fig. 6(a) reveals that decoherence induced by dephasing significantly alters the distinguishability between initial PAGSs, as superimposed algebraic curves for displacement parameters partially overlap the locus of points yielding the highest distinguishability. It can also be observed that the algebraic curve obtained from (38) with $(x, y) = (0, 0) \in \check{\mathcal{Z}}_{h,k}^{+,(\omega_0,\zeta_0)} \cap \mathbb{R}^2$ as the root of $\mathscr{H}_{h,k}(x, y|\boldsymbol{\Theta}^+(\omega_0, \zeta_0))$ still leads to the highest distinguishability. Therefore, the initial PAGSs designed using displacement parameters identified by such a curve remain optimal even in the presence of decoherence.[9]

Figure 6(b) shows the distinguishability between PSGSs affected by decoherence induced by dephasing. Here, compared to Fig. 6(a), the algebraic curves for displacement parameters that make initial PSGSs orthogonal overlap the locus of points yielding the highest distinguishability between PSGSs affected by decoherence. Therefore, the choice of the parameters that make initial PSGSs orthogonal remains optimal even in the presence of decoherence.

Figure 7 presents the distinguishability between PVGSs of different type affected by dephasing. Specifically, Fig. 7(a) (Fig. 7(b)) shows the distinguishability between a noisy PAGS (PSGS) and a noisy PSGS (PAGS), together with the algebraic curves, given by (41), for displacement parameters that make the initial pair of states orthogonal. Analogously to Fig. 6(b), these algebraic curves still provide the optimal design parameters that yield the highest distinguishability between quantum states impaired by decoherence.

Since the developed methodologies can be used for designing maximally distinguishable PVGSs in the presence of decoherence, they can be of practical interest for the implementation of quantum systems that rely on distinguishing quantum states, e.g., quantum sensing and communication systems.

VI. CONCLUSION

This paper explored the distinguishability between PVGSs, a broad class of non-Gaussian states whose inner product depends on generalized HKdF polynomials. We first showed that orthogonalizing PVGSs is tantamount to determining the algebraic varieties of such polynomials, thus bridging the fields of quantum mechanics and algebraic geometry. Subsequently, we proved the existence of orthogonal PVGSs by showing that there exist choices of their parameters that lead to nonempty algebraic varieties. From this finding, we then provided an algebraic interpretation of why Gaussian states are always nonorthogonal. Furthermore, we exploited the geometrical properties of the algebraic varieties to establish methodologies for designing pairs of orthogonal PVGSs, thus overcoming the limitation of Gaussian states. Finally, we explored the distinguishability of PVGSs undergoing noisy time evolution in the presence of quantum decoherence. In such conditions, the developed methodologies can still be leveraged to design maximally distinguishable states. The findings of this paper advance the knowledge on non-Gaussian states and provide insights into designing a new class of quantum states that are distinguishable.

ACKNOWLEDGMENTS

The fundamental research described in this paper was supported, in part, by the Ministero dell'Università e della Ricerca and NextGenerationEU under Grant No. 2022JES5S2, by the National Research Foundation of Korea under Grant No. RS-2024-00409492, and by the Robert R. Taylor Professorship.

[9]This does not hold in general, as orthogonal states can become less distinguishable than states that are not orthogonal.

DATA AVAILABILITY

The data that support the findings of this article are not publicly available. The data are available from the authors upon reasonable request.

APPENDIX A: SURJECTIVITY OF THE FUNCTION η

Lemma A1 (surjectivity of the function η). Let $z_0 \in \mathbb{C}_*$. Then, the function $\eta(\cdot, z_0) : \mathbb{C} \to \mathbb{C}$ is surjective. $\square$

Proof. Let $z_0 \in \mathbb{C}_*$. Proving that $\mathrm{Ran}(\eta(\cdot, z_0)) = \mathbb{C}$ requires proving that $\forall\, w \in \mathbb{C}, \exists\, x \in \mathbb{C} : w = \eta(x, z_0)$. From (10), $\eta(\cdot, z_0)$ is surjective if the complex equation

$$\mathrm{Re}\{w\} + \imath\, \mathrm{Im}\{w\} = \frac{\mathrm{Re}\{x\} + \imath\, \mathrm{Im}\{x\} - (\mathrm{Re}\{x\} - \imath\, \mathrm{Im}\{x\}) \tanh(|z_0|) e^{\imath \angle z_0}}{\sqrt{-2 \tanh(|z_0|)\, e^{\imath \angle z_0}}} \tag{A1}$$

has a solution with respect to the variables $\mathrm{Re}\{x\}$ and $\mathrm{Im}\{x\}$. By splitting real and imaginary parts, Eq. (A1) can be written as the system of real equations

$$\boldsymbol{C}\boldsymbol{x} = \boldsymbol{d},$$

with

$$\boldsymbol{C} \triangleq \begin{bmatrix} 1 - \tanh(|z_0|)\cos(\angle z_0) & -\tanh(|z_0|)\sin(\angle z_0) \\ -\tanh(|z_0|)\sin(\angle z_0) & 1 + \tanh(|z_0|)\cos(\angle z_0) \end{bmatrix},$$

$$\boldsymbol{x} \triangleq \begin{bmatrix} \mathrm{Re}\{x\} \\ \mathrm{Im}\{x\} \end{bmatrix},$$

$$\boldsymbol{d} \triangleq \begin{bmatrix} -\sqrt{2\tanh(|z_0|)}\left[\mathrm{Re}\{w\}\sin\left(\frac{\angle z_0}{2}\right) + \mathrm{Im}\{w\}\cos\left(\frac{\angle z_0}{2}\right)\right] \\ \sqrt{2\tanh(|z_0|)}\left[\mathrm{Re}\{w\}\cos\left(\frac{\angle z_0}{2}\right) - \mathrm{Im}\{w\}\sin\left(\frac{\angle z_0}{2}\right)\right] \end{bmatrix}.$$

By observing that $\det\{\boldsymbol{C}\} = 1 - \tanh(|z_0|)^2 \neq 0$, we can conclude that $\eta(\cdot, z_0)$ is surjective. $\boxtimes$

APPENDIX B: SURJECTIVITY OF THE FUNCTIONS Ψ AND Φ

Lemma B1 (surjectivity of the functions Ψ and Φ onto $\mathbb{R}$). The functions $\Psi : \mathbb{C}^2 \times \mathbb{C}_*^2 \to \mathbb{C}$ and $\Phi : \mathbb{C}^2 \times \mathbb{C}_*^2 \to \mathbb{C}$ are surjective onto $\mathbb{R}$. $\square$

Proof. Proving that Ψ and Φ are surjective onto $\mathbb{R}$ is equivalent to proving that $\exists\, \mathcal{A}, \mathcal{B} \subseteq \mathbb{C}^2 \times \mathbb{C}_*^2, \mathcal{A} \neq \varnothing \neq \mathcal{B}$: $\mathrm{Ran}(\Psi|_{\mathcal{A}}) = \mathbb{R} = \mathrm{Ran}(\Phi|_{\mathcal{B}})$. By taking $\mathcal{A} = \mathbb{R}^2 \times \mathbb{R}_-^2 = \mathcal{B}$ and using Lemma A1 in Appendix A together with (17), it follows that $\mathrm{Ran}(\Psi|_{\mathbb{R}^2 \times \mathbb{R}_-^2}) = \mathbb{R} = \mathrm{Ran}(\Phi|_{\mathbb{R}^2 \times \mathbb{R}_-^2})$, thus concluding the proof. $\boxtimes$

[1] R. J. Glauber, The quantum theory of optical coherence, Phys. Rev. **130**, 2529 (1963).

[2] B. L. Schumaker, Quantum mechanical pure states with Gaussian wave functions, Phys. Rep. **135**, 317 (1986).

[3] C. Weedbrook, S. Pirandola, R. García-Patrón, N. J. Cerf, T. C. Ralph, J. H. Shapiro, and S. Lloyd, Gaussian quantum information, Rev. Mod. Phys. **84**, 621 (2012).

[4] M. Walschaers, Non-Gaussian quantum states and where to find them, PRX Quantum **2**, 030204 (2021).

[5] U. Chabaud, D. Markham, and F. Grosshans, Stellar representation of non-Gaussian quantum states, Phys. Rev. Lett. **124**, 063605 (2020).

[6] U. Chabaud and S. Mehraban, Holomorphic representation of quantum computations, Quantum **6**, 831 (2022).

[7] A. Kenfack and K. Zyczkowski, Negativity of the Wigner function as an indicator of non-classicality, J. Opt. B **6**, 396 (2004).

[8] D. Gottesman, A. Kitaev, and J. Preskill, Encoding a qubit in an oscillator, Phys. Rev. A **64**, 012310 (2001).

[9] N. Shukla, S. Nimmrichter, and B. C. Sanders, Squeezed comb states, Phys. Rev. A **103**, 012408 (2021).

[10] B. Yurke and D. Stoler, Generating quantum mechanical superpositions of macroscopically distinguishable states via amplitude dispersion, Phys. Rev. Lett. **57**, 13 (1986).

[11] A. Ourjoumtsev, R. Tualle-Brouri, J. Laurat, and P. Grangier, Generating optical Schrödinger kittens for quantum information processing, Science **312**, 83 (2006).

[12] K. Takase, J.-i. Yoshikawa, W. Asavanant, M. Endo, and A. Furusawa, Generation of optical Schrödinger cat states by generalized photon subtraction, Phys. Rev. A **103**, 013710 (2021).

[13] A. Giani, M. Z. Win, and A. Conti, Quantum sensing and communication via non-Gaussian states, IEEE J. Sel. Areas Inf. Theory **6**, 18 (2025).

[14] M. He and S. Liu, Performance optimization of continuous-variable quantum teleportation with generalized photon-varying non-Gaussian operations, Phys. Rev. A **110**, 012425 (2024).

[15] S. Guerrini, M. Z. Win, and A. Conti, Photon-varied quantum states: Unified characterization, Phys. Rev. A **108**, 022425 (2023).

[16] M. Dakna, T. Anhut, T. Opatrný, L. Knöll, and D.-G. Welsch, Generating Schrödinger-cat-like states by means of conditional measurements on a beam splitter, Phys. Rev. A **55**, 3184 (1997).

[17] P. Marian and T. A. Marian, A geometric measure of non-classicality, Phys. Scr. **95**, 054005 (2020).

[18] F. Albarelli, M. G. Genoni, M. G. A. Paris, and A. Ferraro, Resource theory of quantum non-Gaussianity and Wigner negativity, Phys. Rev. A **98**, 052350 (2018).

[19] M. Barbieri, N. Spagnolo, M. G. Genoni, F. Ferreyrol, R. Blandino, M. G. A. Paris, P. Grangier, and R. Tualle-Brouri, Non-Gaussianity of quantum states: An experimental test on single-photon-added coherent states, Phys. Rev. A **82**, 063833 (2010).

[20] I. Ghiu, P. Marian, and T. A. Marian, Measures of non-Gaussianity for one-mode field states, Phys. Scr. **2013**, 014028 (2013).

[21] A. Zavatta, S. Viciani, and M. Bellini, Quantum-to-classical transition with single-photon-added coherent states of light, Science **306**, 660 (2004).

[22] K. Wakui, H. Takahashi, A. Furusawa, and M. Sasaki, Photon subtracted squeezed states generated with periodically poled $\mathrm{KTiOPO_4}$, Opt. Express **15**, 3568 (2007).

[23] A. Zavatta, V. Parigi, and M. Bellini, Experimental nonclassicality of single-photon-added thermal light states, Phys. Rev. A **75**, 052106 (2007).
[24] A. Ourjoumtsev, A. Dantan, R. Tualle-Brouri, and P. Grangier, Increasing entanglement between Gaussian states by coherent photon subtraction, Phys. Rev. Lett. **98**, 030502 (2007).
[25] N. Namekata, Y. Takahashi, G. Fujii, D. Fukuda, S. Kurimura, and S. Inoue, Non-Gaussian operation based on photon subtraction using a photon-number-resolving detector at a telecommunications wavelength, Nat. Photonics **4**, 655 (2010).
[26] J. Fadrný, M. Neset, M. Bielak, M. Ježek, J. Bílek, and J. Fiurášek, Experimental preparation of multiphoton-added coherent states of light, npj Quantum Inf. **10**, 89 (2024).
[27] S. Guerrini, M. Z. Win, M. Chiani, and A. Conti, Quantum discrimination of noisy photon-added coherent states, IEEE J. Sel. Areas Inf. Theory **1**, 469 (2020).
[28] P. V. P. Pinheiro and R. V. Ramos, Quantum communication with photon-added coherent states, Quantum Inf. Process. **12**, 537 (2013).
[29] P. Huang, G. He, J. Fang, and G. Zeng, Performance improvement of continuous-variable quantum key distribution via photon subtraction, Phys. Rev. A **87**, 012317 (2013).
[30] N. Akhtar, J. Wu, J.-X. Peng, W.-M. Liu, and G. Xianlong, Sub-Planck structures and sensitivity of the superposed photon-added or photon-subtracted squeezed-vacuum states, Phys. Rev. A **107**, 052614 (2023).
[31] E. Villasenor, M. He, Z. Wang, R. Malaney, and M. Z. Win, Enhanced uplink quantum communication with satellites via downlink channels, IEEE Trans. Quantum Eng. **2**, 1 (2021).
[32] L. Fan and M. S. Zubairy, Quantum illumination using non-Gaussian states generated by photon subtraction and photon addition, Phys. Rev. A **98**, 012319 (2018).
[33] S. Srikara, K. Thapliyal, and A. Pathak, Continuous variable B92 quantum key distribution protocol using single photon added and subtracted coherent states, Quantum Inf. Process. **19**, 371 (2020).
[34] S. Wang, X. Xu, Y. Xu, and L. Zhang, Quantum interferometry via a coherent state mixed with a photon-added squeezed vacuum state, Opt. Commun. **444**, 102 (2019).
[35] J. Li, Z. Li, Z. Sun, L. Zhou, Y. Li, H. Wang, and H. Ma, Phase-matching quantum key distribution with the single-photon-added coherent source, J. Opt. Soc. Am. B **40**, 2108 (2023).
[36] I. Area, D. K. Dimitrov, and E. Godoy, Zero sets of bivariate Hermite polynomials, J. Math. Anal. Appl. **421**, 830 (2015).
[37] G. Dattoli, S. Lorenzutta, G. Maino, and A. Torre, Theory of multiindex multivariable Bessel functions and Hermite polynomials, Matematiche **52**, 177 (1997).
[38] G. Dattoli, Generalized polynomials, operational identities and their applications, J. Comput. Appl. Math. **118**, 111 (2000).
[39] H. M. Srivastava and J. P. Singhal, Some extensions of the Mehler formula, Proc. Am. Math. Soc. **31**, 135 (1972).
[40] R. Loudon, *The Quantum Theory of Light*, 3rd ed. (Oxford University Press, New York, 2000).
[41] H. P. Breuer and F. Petruccione, *The Theory of Open Quantum Systems* (Oxford University Press, Oxford, 2002).
[42] M. Clouâtré, S. Marano, P. L. Falb, and M. Z. Win, Admissible optimal control for parameter estimation in quantum systems, IEEE Control Syst. Lett. **8**, 2283 (2024).